Title

Protein kinase Cζ exhibits constitutive phosphorylation and phosphatidylinositol-3,4,5-triphosphate-independent regulation.

Journal

Biochemical Journal, 473(4)

ISSN

0264-6021

Authors

Tobias, Irene S
Kaulich, Manuel
Kim, Peter K
et al.

Publication Date

2016-02-15

DOI

10.1042/bj20151013

Peer reviewed

HHS Public Access

Author manuscript

Biochem J. Author manuscript; available in PMC 2016 June 01.

Published in final edited form as:

Biochem J. 2016 February 15; 473(4): 509–523. doi:10.1042/BJ20151013.

Protein kinase Cζ exhibits constitutive phosphorylation and phosphatidylinositol-3,4,5-triphosphate-independent regulation

Irene S. Tobias[*,†], **Manuel Kaulich**[‡], **Peter K. Kim**[§], **Nitya Simon**[*], **Estela Jacinto**[§], **Steven F. Dowdy**[‡], **Charles C. King**[||], and **Alexandra C. Newton**[*,1]

[*]Department of Pharmacology, University of California San Diego, La Jolla, CA 92093, U.S.A

[†]Biomedical Sciences Graduate Program, University of California San Diego, La Jolla, CA 92093, U.S.A

[‡]Department of Cellular and Molecular Medicine, University of California San Diego, La Jolla, CA 92093, U.S.A

[§]Department of Biochemistry and Molecular Biology, Rutgers-Robert Wood Johnson Medical School, Piscataway, NJ 08854, U.S.A

[||]Department of Pediatrics, University of California San Diego, La Jolla, CA 92093, U.S.A

Abstract

Atypical protein kinase C (aPKC) isoenzymes are key modulators of insulin signalling, and their dysfunction correlates with insulin-resistant states in both mice and humans. Despite the engaged interest in the importance of aPKCs to type 2 diabetes, much less is known about the molecular mechanisms that govern their cellular functions than for the conventional and novel PKC isoenzymes and the functionally-related protein kinase B (Akt) family of kinases. Here we show that aPKC is constitutively phosphorylated and, using a genetically-encoded reporter for PKC activity, basally active in cells. Specifically, we show that phosphorylation at two key regulatory sites, the activation loop and turn motif, of the aPKC PKCζ in multiple cultured cell types is constitutive and independently regulated by separate kinases: ribosome-associated mammalian target of rapamycin complex 2 (mTORC2) mediates co-translational phosphorylation of the turn motif, followed by phosphorylation at the activation loop by phosphoinositide-dependent kinase-1 (PDK1). Live cell imaging reveals that global aPKC activity is constitutive and insulin unresponsive, in marked contrast to the insulin-dependent activation of Akt monitored by an Akt-specific reporter. Nor does forced recruitment to phosphoinositides by fusing the pleckstrin homology (PH) domain of Akt to the kinase domain of PKCζ alter either the phosphorylation or activity of PKCζ. Thus, insulin stimulation does not activate PKCζ through the canonical phosphatidylinositol-3,4,5-triphosphate-mediated pathway that activates Akt, contrasting with previous literature on PKCζ activation. These studies support a model wherein an alternative

[1]To whom correspondence should be addressed (; Email: anewton@ucsd.edu)

AUTHOR CONTRIBUTION

Irene Tobias and Alexandra Newton conceived the experiments and wrote the manuscript. Irene Tobias performed and analysed the experiments with assistance from Manuel Kaulich and Steven Dowdy on Figure 2(C) and Nitya Simon on Figures 3(A) and 3(B). Peter Kim performed the experiments shown in Figure 5, which were analysed by Peter Kim and Estela Jacinto. Charles King provided advice on experimental design. All authors reviewed the results and approved the final version of the manuscript.

mechanism regulates PKCζ-mediated insulin signalling that does not utilize conventional activation via agonist-evoked phosphorylation at the activation loop. Rather, we propose that scaffolding near substrates drives the function of PKCζ.

Keywords

atypical protein kinase C; insulin; mTOR complex; phosphatidylinositol signalling; phosphatidylserine; phosphorylation

INTRODUCTION

Atypical protein kinase C (aPKC) isoenzymes have been implicated as key modulators of insulin signalling and type 2 diabetes [1–3]. aPKCs are required for insulin-stimulated glucose transport in skeletal muscle and adipocytes [4–7]. The aPKC isoenzymes, PKCζ and PKCι/λ (PKCι is the human orthologue of mouse PKCλ) can function interchangeably to regulate glucose transport [8], although they exhibit species-specific differential expression [3]. Knockout of PKCλ (the predominant aPKC isoenzyme expressed in mice [9]) in embryonic stem cells and adipocytes impairs insulin-stimulated glucose transport [10]. Mice with muscle-specific knockout of PKCλ also exhibit metabolic and diabetic syndromes [11]. Furthermore, the activity of aPKC immunoprecipitated from skeletal muscle or adipocyte tissues of obese humans or patients with type 2 diabetes is non-responsive to prior treatment of the tissue with insulin [12–14], yet aPKC is hyperactive in liver tissue of rodents and humans with type 2 diabetes [15,16]. Hepatic aPKC is known to activate lipogenic and pro-inflammatory pathways [17,18], further exacerbating disease. Indeed, pharmacological inhibition of aPKC in the liver has been proposed as a treatment for type 2 diabetes and metabolic syndrome [2]. Despite the heightened interest in the role and drugability of aPKC in metabolic disease, much less is understood about the molecular mechanisms that drive the cellular functions of aPKCs compared with other PKCs.

aPKCs are classified as one of the three subfamilies of the PKC Ser/Thr protein kinases. However, unlike the other two classes (conventional and novel), aPKCs are not regulated by diacylglycerol. Conventional PKC (cPKC) and novel PKC (nPKC) isoenzymes sense diacylglycerol via a C1 domain, and although atypical PKCs have a C1 domain, it lacks determinants that allow the binding of diacylglycerol [19,20]. Nor are they regulated by Ca^{2+}, a defining feature of conventional PKCs that is mediated by a Ca^{2+}-sensing C2 domain. In place of second messenger-sensing modules, atypical PKCs have a protein-binding PB1 domain at their regulatory N-terminus and a PDZ ligand at the C-terminus [21,22]. They also have an autoinhibitory pseudosubstrate segment shared by all PKCs. In order for aPKCs to be active, this pseudosubstrate must be removed from the substrate-binding cavity, an event that can occur upon binding to protein scaffolds such as PAR6 [23] and p62 [24]. The aPKC isoenzyme PKCζ has an alternate transcript (PKMζ) preferentially expressed in brain tissue that contains the catalytic domain and lacks all N-terminal regulatory domains (PB1, pseudosubstrate and atypical C1). The lack of second messenger-responsive regulatory moieties of aPKCs sets them apart from cPKCs and nPKCs. Indeed, their position on the kinome tree places them halfway between protein kinase B (Akt) and

the other PKCs [25], suggesting they should be considered as a separate family in the kinome.

Phosphorylation plays a key role in regulating all PKCs. cPKC and nPKC isoenzymes have three priming phosphorylation sites: the activation loop present near the ATP-binding site, and two sites present in the C-terminal tail, the turn motif and the hydrophobic motif [21]. aPKCs share the first two sites, but a phosphomimetic Glu occupies the phospho-acceptor position in the hydrophobic motif site; this unique feature of aPKCs renders them insensitive to dephosphorylation by the phosphatase PHLPP which dephosphorylates this site on Akt [26] and on other PKCs leading to their inactivation and down-regulation, respectively [27–29]. The activation loop of all PKCs and the related family of Akt kinases are phosphorylated by PDK1 [30–32]. Phosphorylation at the activation loop is constitutive for cPKC and nPKC isoenzymes and is likely the first phosphorylation event in the maturation of these PKCs [22]. However, phosphate at the activation loop becomes dispensable for activity in cPKC isoenzymes once the kinases are fully phosphorylated [33]. For Akt, phosphorylation at the PDK1 site is agonist evoked.

The regulation of activation loop phosphorylation in aPKCs is unclear. Previous studies proposed that activation loop phosphorylation by PDK1 on aPKC isoenzymes is agonist-evoked and leads to increased activity upon insulin stimulation [34–36]. Indeed, the literature commonly cites the activation of aPKC to be analogous to the mechanism of Akt activation in which agonist-stimulated PIP_3 production by phosphoinositide 3-kinase (PI3-K) evokes Akt translocation to the plasma membrane (PM) where its autoinhibitory pleckstrin homology (PH) domain binds to PIP_3 and permits activation loop phosphorylation by PDK1 [37,38]. However, multiple studies also report data showing that insulin stimulation does not affect activation loop phosphorylation on aPKC in immortalized cell lines [39], primary rat hepatocytes [40], and even in biopsied human muscle tissue following insulin injection *in vivo* [41]. Thus, whether the activation loop phosphorylation of aPKCs is agonist-dependent, as it is for Akt, or constitutive, as it is for cPKCs, remains to be resolved.

The role and mechanism of phosphorylation for the turn motif of aPKCs are unclear. For cPKCs, phosphorylation at this site is necessary to stabilize the enzyme in a catalytically-competent conformation [42]; loss of phosphorylation at this site inactivates the enzyme [33,43,44]. The mTORC2 is required for the phosphorylation of the turn motif site in both PKC and Akt, however by different mechanisms [39,45,46]. For Akt, mTORC2 directly phosphorylates the nascent Akt polypeptide as it emerges from the ribosome [47,48]. In contrast, cPKC isoenzymes are phosphorylated post-translationally, with a half-time on the order of 15 min, and at a membrane fraction [49,50]. Although mTORC2 is required for PKC to become phosphorylated [46,51], whether it directly phosphorylates the turn motif of cPKC or indirectly regulates the site by activation of another kinase or chaperoning remains to be established. The first phosphorylation of cPKCs is the PDK1-mediated phosphorylation on the activation loop, which is a prerequisite for phosphorylation of the turn motif [30,33]. The turn motif of aPKC has been proposed to be regulated by autophosphorylation subsequent to activation loop phosphorylation [6,35], similar to the hydrophobic motif autophosphorylation of cPKC [52]. However, evidence for this claim is

also controversial, with recent studies identifying mTORC2 as responsible for phosphorylating the turn motif of aPKC [39].

Given the incomplete understanding of how aPKC isoenzymes are regulated, we set out to examine the regulation of PKCζ by phosphorylation, insulin and lipids. Our data reveal that PKCζ is processed by two ordered phosphorylations: the nascent enzyme is co-translationally phosphorylated by ribosome-localized mTORC2 followed by PDK1-catalysed phosphorylation at the activation loop to yield a constitutively-phosphorylated and catalytically-competent enzyme. The phosphorylations are stable and insensitive to both insulin and PIP_3. Live cell imaging using a genetically-encoded reporter to measure cellular PKC activity reveals no detectable basal or insulin-stimulated activity on a cytosolic substrate. Based on the exceptionally low turn-over of PKCζ (on the order of five reactions per minute), our data support a model in which a mechanism other than phosphorylation is responsible for activating PKCζ, probably involving conformational changes and opportunistic localization towards substrates via protein scaffolds.

EXPERIMENTAL

Materials

Calyculin A, staurosporine and LY294002 were purchased from Calbiochem. OSU-03012 was acquired from Cayman Chemical Co. Torin 1 was purchased from Tocris, and GDC-0068 was acquired from Selleckchem. Insulin and cyclohexamide were purchased from Sigma. PZ09 was a kind gift from Dr Sourav Ghosh and Dr Christopher Hulme. The following antibodies were purchased from Santa Cruz Biotechnology: anti-p410 PKCζ (sc-12894-R), anti-total PKCζ (sc-216), anti-rpL23a (sc-130252) and anti-GST (sc-138). Antibodies for p308 Akt (9275), p450 Akt (9267), p473 Akt (4060), total Akt (9272), PDK1 (3062), GAPDH (2118), mTOR (2983), rpS6 (2317) p389 ribosomal protein S6 kinase (S6K) (9205), total S6K (9202) and GFP (2555) were purchased from Cell Signaling Technology. The anti-p560 PKCζ antibody was purchased from AbCam (ab62372), the anti-haemagglutinin (HA) antibody was from Covance (MMS-101P) and the anti-actin antibody was from Sigma (A2228). HRP-conjugated goat anti-mouse IgG and goat anti-rabbit IgG were from Calbiochem (401215 and 401315). AlexaFluor 488-conjugated goat anti-rabbit IgG was from Invitrogen (A110034). Phosphatidylserine (PS), PIP_3 and phosphatidylinositol-4,5-biphosphate (PIP_2) were purchased from Avanti Polar Lipids (840034, 850457, 850156 and 850155, respectively). Phosphatidic acid (PA) was purchased from Santa Cruz Biotechnology (201059).

Cell lines and plasmid constructs

The PDK1−/− and +/+ murine embryonic fibroblasts (MEFs) were generously provided by DrWataru Ogawa, Dr Feng Liu and Dr Kun-Liang Guan. The stress-activated map kinase-interacting protein 1 (Sin1)−/− and +/+ MEFs were also a gift from Dr Kun-Liang Guan. The Hep1C1C7 mouse liver cells were a gift from Dr Jerry Olefsky. Human PKCζ cDNA was a gift from Dr Tony Hunter whereas human Akt2 cDNA was a gift from Dr Alex Toker. The C-kinase activity reporter (CKAR), B-kinase activity reporter (BKAR) and plasma membrane-targeted CFP (PM-CFP) constructs were described previously [53,54]. The

pFastBac HT/B vector (Invitrogen) was modified in-house to insert a GST tag for purification in place of the His tag preceding the TEV cleavage site. The first 151 amino acids of human Akt2 were fused to human PKMζ (residues 184–592 of PKCζ) to construct the Akt2R-PKMζ chimaeric kinase. Human PKCζ, Akt2 and Akt2R-PKMζ constructs were cloned into the pDONR221 vector and subsequently recombined with various pDEST vectors constructed in-house to make fusion proteins with HA, mCherry or yellow fluorescent protein (YFP) tags at the N-terminus in pcDNA3 vectors for mammalian cell expression or N-terminal GST-tagged constructs in pFastBac vector for insect cell expression using the Gateway cloning system (Invitrogen). Point mutations were made using Quikchange site-directed mutagenesis (Stratagene).

Baculovirus construction and purification of PKCζ

Baculoviruses were made in Sf-9 insect cells from pFastBac plasmids using the Bac-to-Bac expression system (Invitrogen). Batch purification using glutathione sepharose beads was used to purify the GST-tagged proteins from infected Sf-9 insect cell cultures. Briefly, cells were rinsed with PBS and lysed in 50 mM HEPES pH 7.5, 100 mM NaCl (Buffer A) with 0.1% Triton X-100, 100 μM PMSF, 1 mM DTT, 2 mM benzamidine and 50 μg/ml leupeptin. The soluble lysate was incubated with glutathione resin beads for 30 min at 4°C. Protein-bound beads were washed three times in Buffer A and then eluted three times in Buffer A with 10 mM glutathione. Eluent was loaded in a 30 kDa Amicon centrifugal filter unit (EMD Millipore) and washed/concentrated three times with Buffer B (20 mM HEPES, pH 7.4, 0.1 mg/ml BSA, 2 mM DTT). Glycerol was added to 50% volume before measurement of PKCζ concentration using BSA standards on a Coomassie Brilliant Blue stained gel and storage of enzyme stocks at −20°C. We note that absolute PKCζ concentrations may not be accurate using BSA as standards.

Lipid stock preparation

PIP_3 and PIP_2 were dissolved in 80% chloroform and 20% methanol, whereas all other lipids were dissolved in 100% chloroform. Lipid mixtures were dried under nitrogen gas and then rehydrated in 20 mM Tris, pH 7.4 (for PS, PC and PA) or water (for PIP_3 and PIP_2) and sonicated to form 10× stocks. For Triton X-100 micelle systems, dried lipids were dissolved in 1% protein-grade Triton X-100 (Calbiochem) and diluted to form different 10× mol% lipid formulations.

In vitro kinase activity assay

Purified or immunoprecipitated proteins were diluted in Buffer B. Kinase activity was measured in 80 μl reactions supplemented with 140 μM PS for standard multilamellar assay or 10× lipid/Triton X-100 formulation for mixed micelle assays. aPKC reactions were initiated by addition of 100 μM ATP, 100 μg/ml myelin basic protein (MBP, Sigma), 5 mM $MgCl_2$ and 10 μCi/ml [γ-^{32}P]ATP (PerkinElmer). Reactions were conducted for 15–30 min at 30°C with 20–25 nM enzyme for purified proteins, stopped by addition of 25 mM ATP, 25 mM EDTA, pH 8.0, and spotted on to P81 Whatman filters. Filters were washed 4× with 0.4% phosphoric acid before measurement using a Beckman scintillation counter.

In vitro phosphatase assay

25 nM purified GST-PKCζ was incubated in Buffer B with 140 μM PS, 200 μM $MnCl_2$, 500 μM $CaCl_2$, 400 μM EDTA and 100 units/ml protein phosphatase 1 (PP1, New England Biolabs) for 0–60 min at 30°C in 40 μl reactions. Reactions were stopped at various time points with Buffer C (62.5 mM Tris, 2% SDS, 10% glycerol, 20 μg/ml Bromophenol Blue, 2.86 M 2-mercaptoethanol) with 5 mM EDTA then run on immunoblots to quantify dephosphorylation of GST-PKCζ over time.

Cell culture and transfection

Sf-9 cells were grown in Sf-900 II SFM media (Gibco) in shaking cultures at 27°C. All mammalian cells were maintained at 37°C in 5% CO_2. Chinese hamster ovary cell overexpressing insulin receptor (CHO-IR) cells were grown in DMEM/F-12 50/50, 1× (Cellgro) supplemented with 5% dialysed fetal bovine serum (FBS, Atlanta Biologics), 100 units/ml penicillin, 100 μg/ml streptomycin and 50 μg/ml geneticin (Gibco). Hep1C1C7 cells were grown in MEM Alpha 1X (Gibco) supplemented with 10% FBS, 100 units/ml penicillin and 100 μg/ml streptomycin. COS-7, 293T and all MEFs were grown in DMEM 1× supplemented with 10% FBS, 100 units/ml penicillin and 100 μg/ml streptomycin. 3 μg/ml puromycin (Sigma) was added to the media for PDK1+/+ and −/− MEFs. Mammalian cells were transiently transfected using jetPrime (Polyplus Transfection).

Immunoprecipitation and immunoblotting

Cells transfected with HA-tagged kinases to be immunoprecipitated were serum starved overnight and treated with or without 100 nM insulin (Sigma) for 10 min before rinsing in PBS and lysing in Buffer D (100 mM KCl, 50 mM Tris, 3 mM NaCl, 3.5 mM $MgCl_2$, pH 7.3) with 1% protein-grade Triton X-100 (Calbiochem), 100 μM PMSF, 1 mM DTT, 2 mM benzamidine, 50 μM PMSF, 50 μg/ml leupeptin, 1 μM microcystin-LR (Calbiochem) for activity assays or Buffer E (150 mM NaCl, 50 mM Tris, 100 mM NaF, 100 mM β-glycerophosphate, 1% IGEPAL pH 7.8) with 20 μg/ml RNaseA, 20 μg/ml DNaseI, phosphatase inhibitor cocktails #2 and #3 diluted 1:100 (Sigma, P5726 and P0044) and protease inhibitor cocktail diluted 1:200 (Sigma, P8340) for immunoprecipitation (IP) prior to isoelectric focusing (IEF). Soluble lysates were incubated with anti-HA antibody (Covance) for 1–2 h followed by incubation with Protein A/G resin beads (Thermo Scientific) for 1–2 h. Protein-bound beads were washed three times with Buffer D and diluted in Buffer B before assaying activity or were washed three times with Buffer E, PBS, and 1 mM EGTA, 75 mM KCl, 50 mM Tris pH8.5 prior to elution for IEF. For experiments with immunoblotting only, cells were lysed in Buffer F (100 mM NaCl, 50 mM Tris, 10 mM $Na_4P_2O_7$, 50 mM NaF, 1% Triton X-100, pH 7.2) with 100 μM PMSF, 1 mM DTT, 2 mM benzamidine, 50 μM PMSF, 50 μg/ml leupeptin, 1 μM microcystin-LR, and whole cell lysates were sonicated prior to adding Buffer C, boiling at 100°C and performing SDS-PAGE. Gels were transferred to PVDF membrane and blocked with 5% milk before incubating with antibodies and imaging via chemiluminescence on a FluorChemQ imaging system (Protein Simple).

Isoelectric focusing

2D-IEF was performed as described [55] by immunoprecipitating HA-PKCζ and eluting in 7 M urea, 2 M thiourea, 2% CHAPS (pH 8.4), then loading on to the acidic end of 3–10 immobiline strips (GE Healthcare) with the current ramped up from 200 V for 2 h, 500 V for 1 h, 800 V for 1 h, 1000 V for 0.5 h, 1200 V for 0.5 h, 1400 V for 0.5 h, 1600 V for 0.5 h, 1800 V for 2.5 h and 2000 V for 2.5 h. Second dimension was performed by soaking IEF strip in 2% SDS, 6 M urea, 75 mM Tris (pH 8.8), 29% (wt/vol) glycerol, 10 mg/ml DTT and 25 mg/ml iodoacetamide (Sigma–Aldrich), and placing the strip on top of a SDS/10% PAGE containing a single large well to accommodate the IEF strip with molecular weight marker side wells.

Cell fractionation and polysome analysis

Cells were grown, serum starved overnight, re-stimulated with 10% serum for 1 h, treated with 100 mg/ml cyclohexamide for 15 min, then harvested, lysed and processed for fractionation as previously described [47] with the following modification: lysates were layered on a 10 ml 7–47% (w/v) sucrose gradient (five layers: 7, 17, 27, 37, 47%). Fractions were concentrated to a final volume of 100 μl with Amicon Ultra-4 centrifugal filter unit (EMD Millipore). Proteins were separated by SDS-PAGE and detected by immunoblotting.

Live cell fluorescence imaging

COS-7 cells were plated on to sterilized glass coverslips in 35 mm dishes, co-transfected with the indicated constructs, and imaged in Hanks' balanced salt solution supplemented with 1 mM $CaCl_2$ approximately 24 h post-transfection. For experiments with insulin stimulation, cells were serum starved for 4–6 h or overnight prior to imaging via a 40× objective. Kinase activity was monitored via intramolecular FRET of the activity reporters (CKAR or BKAR) whereas kinase translocation was monitored via intermolecular FRET between the YFP-tagged kinase and the PM-CFP using methods previously described [56].

Immunofluorescence

COS-7 cells were seeded on to 22 mm poly-D-lysine-treated glass coverslips in a 6-well plate, grown for approximately 20 h, serum starved for 4 h, and treated with or without 100 nM insulin for 10 min. Cells were rinsed briefly in PBS and fixed with 4% paraformaldehyde for 15 min at room temperature followed by incubation with 100%methanol for 3 min at −20°C. Cells were rinsed again in PBS three times followed by permeabilization and blocking in PBS containing 0.25% Triton X-100, 5% BSA and 5% goat serum for 15 min at room temperature. Cells were incubated in a humidified chamber for 1 h at room temperature with either a PKCζ-specific antibody (Santa Cruz Biotechnology sc-216 diluted 1:40, also detects PKCλ) or a pan-Akt antibody (Cell Signaling 9272, diluted 1:200). Cells were then rinsed three times in PBST and incubated in a humidified chamber protected from light for 30 min at room temperature with an AlexaFluor 488-conjugated secondary antibody (Invitrogen A110034, diluted 1:500). Cells were rinsed a final three times in PBST prior to mounting the coverslips on glass slides and imaging via a 40× objective on a Zeiss Axiovert fluorescent microscope (Carl Zeiss Microimaging) using a

MicroMax digital camera (Roper-Princeton Instruments) controlled by MetaFluor software version 3.0 (Universal Imaging).

Statistical analysis

All statistical analyses were performed using GraphPad Prism 6.0 (GraphPad Software).

RESULTS

Phosphorylation at the activation loop and turn motif of PKCζ is each independently required but not sufficient for activity

Similar to conventional and novel PKC isoenzymes and to Akt, the atypical PKCζ has a Thr residue at the phospho-acceptor site of the conserved activation loop and turn motif. However, contrasting with these closely related enzymes, it contains a phosphomimetic Glu at the hydrophobic motif, a property shared by PKN family members, which have an Asp at this position (Figure 1A). To validate the requirement of phosphorylation at the key conserved Thr residues for enzyme activity using purified protein, rather than immunoprecipitated protein [35], we constructed phospho-resistant Ala mutants at both the activation loop (T410) and the turn motif (T560) of human PKCζ (analogous site locations shown on structure of PKCι in Figure 1B). We purified an N-terminally tagged GST fusion construct of PKC from Sf-9 insect cells. Protein purity of >90% was achieved, with yields on the order of 50 μg protein from 5×10^7 cells for wild-type (WT) enzyme and corresponding mutants (Figure 1C). WT enzyme had a specific activity of 5 ± 1 mol phosphate/min per mol PKC with lipid present (Figure 1D), over an order of magnitude lower than that of conventional PKCs, which catalyse approximately 200 reactions per min with lipid present [57]. Both the T410A and T560A mutants had significantly reduced activity compared with the WT enzyme, with the T560A mutation being even more detrimental to catalytic competency (Figure 1D), in agreement with previous studies conducted on immunoprecipitated versions of these mutants [35]. Consistent with the lack of T410A and T560A mutants' activity, *in vitro* dephosphorylation of WT enzyme with PP1 decreased its activity (data not shown). Mutation of either site to negatively charged phospho-mimetic Glu (T410E or T560E) resulted in a slightly reduced specific activity that was more comparable to that of WT enzyme. The Glu residue present at the hydrophobic motif (E579) was also mutated to Ala to assess the requirement of negative charge at the hydrophobic motif on activity. The E579A mutant had similar activity to WT protein (Figure 1D).

The turn motif (T560) of PKCζ is not regulated by autophosphorylation

To address whether T560 is an autophosphorylation site as previously proposed [6,35], we constructed a catalytically-inactive 'spine mutant' V266F in the kinase domain of PKCζ (conserved alignment with other AGC kinases shown in Figure 1A, structural location in relation to other key sites shown in Figure 1B). This Val residue was mutated to a Phe capable of inserting into the ATP-binding pocket of the enzyme and blocking ATP binding, a method for inactivating a kinase without compromising its structural integrity, recently developed by Taylor et al. [58]. Indeed, the V266F mutant was catalytically dead (Figure 1D) yet was fully phosphorylated at T560 as demonstrated by Western blot analysis of

mammalian CHO-IR lysates expressing this construct (Figure 1E). The specificity of the phospho-specific antibodies was confirmed and validated by the lack of significant labelling of the T410A or T410E constructs by the p410 antibody and the T560A or T560E constructs by the p560 antibody (Figure 1E). Note that replacement of the activation loop with Ala did not affect phosphorylation of the turn motif nor did replacement of the turn motif site with Ala affect phosphorylation of the activation loop. The phosphorylation of the V266F mutant at the turn motif reveals that the intrinsic catalytic activity of PKCζ is not required for phosphorylation of the turn motif.

Phosphorylation at the activation loop (T410) and turn motif (T560) of PKCζ is basal and insensitive to phosphatase inhibition

To assess whether the key phospho-sites of PKCζ are phosphorylated under basal conditions, COS-7 cells were treated with the phosphatase inhibitor calyculin A (50 nM) and phosphorylation was monitored via immunoblotting for a time course up to 10 min after treatment. As a control for phosphatase inhibition, phosphorylation at the hydrophobic motif of S6 kinase (S6K, T389, an agonist-induced phosphorylation site) was monitored and steadily increased over the time period (Figures 2A and 2B). Quantification of data from four separate experiments revealed no change in the phosphorylation state of T410 or T560 following treatment with calyculin (Figure 2B). These data reveal that phosphorylation of PKCζ at the activation loop and turn motif is insensitive to calyculin, reflecting either stoichiometric phosphorylation under basal conditions or regulation by calyculin-insensitive phosphatases. To further investigate the basal phosphorylation state at T410 and T560, 2D IEF was performed on WT HA-PKCζ, single phosphorylation site mutants T410A, T560A and double phosphorylation site mutant T410A T560A immunoprecipitated from CHO-IR cells (Figure 2C). Phosphorylation is a highly acidic modification that is readily resolved by 2D IEF. WT HA-PKCζ enzyme migrated predominantly as two acidic species. Quantification of the data from three independent experiments revealed that the most acidic species comprised 41 ± 2% of the signal. This species probably represents enzyme phosphorylated at both T410 and T560. An intermediate species resolved at the same isoelectric point as each of the single mutants (T410A and T560A) and probably represents a mono-phosphorylated species. A few times, we observed the intermediate species of the WT enzyme separate into a third species (data not shown) that resolved at the same isoelectric point as theT410A T560A double mutant. This spot probably represents enzyme that was dephosphorylated during the IP process. These data reveal that doubly phosphorylated PKCζ is a significant species in cells.

Phosphatidylserine promotes the open conformation of PKCζ, as evidenced by increased rate of dephosphorylation at T410 on PKCζ, and increases specific activity of purified PKCζ; low concentrations of phosphoinositides do not activate PKCζ

For conventional PKC isoenzymes, binding to activating lipids promotes an open conformation that results in a two-orders of magnitude increase in phosphatase sensitivity at their priming sites [33]. To investigate whether binding to PS, which binds the C1 domain of all PKCs [59] also induces an open conformation of PKCζ, we examined the effect of PS on the rate of dephosphorylation of PKCζ. Purified GST-PKCζ was incubated *in vitro* with PP1, a phosphatase known to dephosphorylate both the activation loop and turn motif of PKC

isoenzymes [33]. The rate of dephosphorylation at T410 was measured through quantitative immunoblots and was significantly increased in the presence of PS lipid (Figures 3A and 3B). To assess the effect of lipids on the specific activity of PKCζ, we employed two different *in vitro* lipid systems: multilamellar structures and Triton X-mixed micelles, used previously to examine the effects of lipids on the activity of conventional PKC [57,60,61]. The abundant lipids PS and PA were prepared as multilamellar structures whereas the rare lipids PIP_3 and its PI3-K-targeted precursor PIP_2 were solubilized with Triton X-100 to form mixed micelles with varying mole percent lipid, illustrated by cartoons in Figure 3(C). The latter system is particularly useful in examining lipid specificity and stoichiometry for activation of monomeric PKC [62–64]. The specific activity of GST-PKCζ was increased nearly 3-fold with increasing PS multilamellar concentrations up to 140 μM; PA multilamellar activated PKCζ to a more modest extent (Figure 3D). Neither PIP_3 nor PIP_2 activated PKCζ at concentrations up to 2.5 mol% (corresponding to 3–4 molecules of the lipid per micelle) in the mixed micelle system (Figure 3E) revealing these lipids are not acting as specific agonists for PKCζ. Higher concentrations were not tested given the low abundance of these lipids in membranes. These data support previous findings that the activity of PKCζ is stimulated by cellular PS but suggest that phosphoinositides and most notably PIP_3 do not stimulate the activity of PKCζ in cells, given the low abundance of these lipids.

PDK1 is required for constitutive phosphorylation of the PKCζ activation loop but not the turn motif

PDK1 phosphorylates the activation loop of PKCζ [30–32], but whether this event is required for phosphorylation of the turn motif is unclear. We examined lysates from PDK1 knockout MEFs (PDK1−/−) compared with their WT (PDK1+/+) counterparts (Figure 4A). As expected, PKCζ from the PDK1 knockout MEFs had significantly reduced T410 phosphorylation compared with the PKCζ in the WT MEFs. In contrast, phosphorylation at T560 was not decreased in the PDK1−/− MEFs, quantification shown in Figure 4(B). We also examined the insulin sensitivity of PKCζ phosphorylation. Treatment of either WT or PDK1−/− MEFs with insulin had no effect on the phosphorylation of either the PDK1 site, T410, or the turn motif, T560 (Figure 4A). As a control, we examined Akt, whose activation loop (T308) phosphorylation is insulin dependent and regulated by PDK1, and was indeed ablated in the PDK1−/− MEFs. Treatment of the PDK1+/+ MEFs with insulin produced a significant increase in T308 Akt phosphorylation, which was blocked by pre-treatment with the general kinase inhibitor staurosporine and reduced by pre-treatment with PDK1-specific inhibitor OSU03012 (Figure 4C). Thus, under conditions where insulin regulates the phosphorylation of the activation loop of Akt, the phosphorylation of the PKCζ activation loop was insensitive to insulin. This result was also observed in the insulin-sensitive CHO-IR cell line (Figure 4D). Taken together, these data reveal that the activation loop of PKCζ is constitutively phosphorylated by PDK1 and that this reaction is not necessary for turn motif phosphorylation.

mTORC2 is required for constitutive phosphorylation of the PKCζ turn motif but not the activation loop

mTORC2 has previously been shown to be required for phosphorylation at the turn motif sites on both conventional PKC and Akt [46], with a recent study also supporting its phosphorylation of the turn motif of PKCζ [39]. To address whether this phosphorylation is necessary for phosphorylation of the PDK1 site, we examined lysates from MEFs that are deficient in Sin1, a necessary component for mTORC2 formation [65]. Phosphorylation at T560 was ablated in Sin1−/− MEFs (Figure 4E) whereas phosphorylation of T410 was comparable between Sin1+/+ MEFs and Sin1−/− MEFs, as quantified in Figure 4(B). Phosphorylation of T560 was unaffected by a 1 h treatment with an mTOR inhibitor, Torin 1, in Sin1+/+ MEFs (Figure 4F) yet was significantly reduced by Torin 1 treatment after 24 h, in agreement with previous studies using long-term mTOR inhibition [39]. In contrast, the phosphorylation at T389 on S6K, the agonist-evoked site of mTORC1 phosphorylation [66], was blocked within 1 h, thus validating mTOR inhibition (Figure 4F). These data reveal that phosphorylation at the turn motif is also constitutive and not necessary for phosphorylation at the PDK1 site.

The phosphorylation of PKCζ at the turn motif but not the activation loop occurs during translation

Previous studies have established that the turn motif of Akt (T450) is phosphorylated during translation, an event that precedes subsequent agonist-evoked phosphorylation of the activation loop (T308) and hydrophobic motif (S473) [47]. These results were acquired by immunoblot analysis of polysomes obtained by fractionation of serum-starved and re-stimulated cells treated with cyclohexamide to preserve intact polysomes. Similar fractionations (Figure 5A) revealed that the PKCζ associated with polysomes is phosphorylated at the turn motif (p560) but not the PDK1 site (p410) (Figure 5B, polysome fractions 7–9). Polysome fractions were devoid of significant PDK1 but had readily detectable levels of mTOR. These data reveal that similar to Akt, the turn motif of PKCζ is co-translationally phosphorylated by mTORC2 at polysomes.

The catalytic activity of PKCζ does not increase following insulin stimulation

We employed both *in vitro* and live cell methods to investigate whether insulin stimulates the intrinsic catalytic activity of PKCζ. Using the *in vitro* assay with MBP as a substrate that we previously validated with pure GST-PKCζ (Figure 1D), we measured the relative catalytic activity of over-expressed HA-PKCζ immunoprecipitated from Hep1C1C7 liver cells treated with or without 100 nM insulin for 10 min. The T560A catalytically-inactive mutant was employed as a control for background kinase activity from the immunoprecipitate. Figure 6(A) shows that WT HA-PKCζ had significantly higher activity than the T560A mutant yet there was no significant difference in activity of enzyme immunoprecipitated from cells treated with or without insulin. We also examined the phosphorylation state of the immunoprecipitated protein and observed no changes in the phosphorylation of the activation loop of PKCζ (p410, Figure 6B). Under the conditions of these assays, insulin caused a robust increase in the activation loop phosphorylation of endogenous Akt (p308). Similar results were also observed in insulin-sensitive CHO-IR cells (data not shown). Using

a genetically-encoded FRET reporter, CKAR [53] previously validated for examining activity of the PKCζ catalytic moiety, PKMζ in real time in live cells [67], we measured the activity of N-terminally tagged mCherry-PKCζ in live COS-7 cells. Insulin treatment did not stimulate PKCζ activity as assessed using CKAR. Under comparable conditions, insulin effectively stimulated Akt activity in cells expressing mCherry-Akt2 as assessed using the Akt reporter BKAR [54]; this activity was reversed with the Akt active site inhibitor GDC-0068 (Figure 6C). Endogenous Akt activity was also stimulated by insulin in cells expressing mCherry vector with BKAR and inhibited by treatment with GDC-0068. Similar results were obtained using a C-terminally tagged PKCζ-RFP construct, examining either cytosolic CKAR or PM-targeted CKAR, in both COS-7 and CHO-IR cells (data not shown).

The phosphorylation of PKCζ is neither agonist evoked nor regulated by PI3-kinase through translocation to the plasma membrane in response to insulin

Previous studies have suggested that PI3-K mediates agonist-evoked phosphorylation of aPKCs by recruiting the enzymes to the membrane through production of PIP_3 in a similar fashion to the activation of Akt [32,35,68,69]. To address this claim, we treated Hep1C1C7 cells with 20 μM of the PI3-K inhibitor LY294002 (LY) prior to insulin stimulation (Figure 7A). No change in T410 or T560 PKCζ phosphorylation was observed with either insulin or LY treatment for either cell line quantified over eight separate experiments (Figure 7B). Similar results were seen with CHO-IR cells under the same conditions (data not shown). As a control, immunoblot analysis revealed that LY abolished the robust insulin-dependent phosphorylation of T308 on Akt. To directly assess whether PKCζ was recruited to the PM in response to insulin treatment, we monitored changes in intermolecular FRET between N-terminally-tagged YFP-PKCζ or YFP-Akt2 and PM-CFP (PM-CFP) in live COS-7 cells during treatment with 100 nM insulin. YFP-Akt2 exhibited a translocation response that was evident through the steady increase in FRET ratio following treatment with insulin (Figure 7C). However, the traces for YFP-PKCζ remained flat after insulin stimulation, indicating that no translocation to the PM had occurred for PKCζ. To corroborate that endogenous PKCζ and Akt displayed the same translocation results as their overexpressed counterparts imaged in Figure 7(C), we performed immunofluorescence imaging of COS-7 cells treated with or without insulin, fixed and stained with antibodies against PKCζ or Akt. The representative images shown in Figure 7(D) reveal a classic PM translocation of Akt in response to insulin, evident through the ruffled appearance of stained Akt in comparison with the untreated control, similar to translocation images from COS7 shown previously [70]. However, no change in the localization of endogenous PKCζ was observed in any of the images taken.

A fusion construct of the Akt2 PH domain with PKMζ translocates to the plasma membrane in response to insulin yet does not exhibit agonist-evoked activity nor phosphorylation at the activation loop

The PH domain of Akt is a well-characterized binder of activated PIP_3 lipid at the PM [71,72]. To investigate whether this domain was also capable of generating aPKC agonist-induced translocation, we fused the regulatory portion of Akt2 that contains the PH domain to the catalytic portion of PKCζ (PKMζ, thus lacking the N-terminal regulatory domains of PKCζ), constructing the chimaeric kinase Akt2R-PKMζ (Figure 8A). Using the PM

translocation assay from Figure 7(C), we monitored translocation of YFP-tagged Akt2R-PKMζ to PM-CFP in live COS-7 cells during treatment with 100 nM insulin compared with YFP-Akt2 and YFP-PKCζ controls. YFP-Akt2R-PKMζ translocated to PM in response to insulin slightly slower than YFP-Akt2 (half-times of 3.01 ± 0.05 min and 2.7 ± 0.1 min, respectively). Note a greater level of steady-state binding was achieved by the chimaera, likely because intramolecular interactions of the PH domain with its native partner Akt kinase domain, but not the foreign aPKC kinase domain, restrain accessibility of the Akt PH domain (Figure 8B); consistent with this, the isolated PH domain translocated to a similar extent as that of the chimaeric kinase (data not shown). We next examined insulin-induced activity of Akt2R-PKMζ on CKAR, using the activity assay from Figure 6(C). mCherry-tagged Akt2R-PKMζ did not exhibit increased activity on cytosolic CKAR following insulin treatment but was basally active on CKAR as shown by the decrease in FRET ratio following inhibition with the aPKC active site inhibitor PZ09, previously characterized to selectively inhibit aPKC over other PKCs *in vitro* [73] (Figure 8C). The control of mCherry-Akt2 showed insulin-induced activity on BKAR although the control for background CKAR activity (mCherry-Vec) was minimally responsive to treatment with 5 μM PZ09. Finally, given that the translocation of Akt2R-PKMζ to PM in response to PIP_3 production could potentially localize the kinase domain of PKCζ to be more opportunistically phosphorylated at its activation loop by PDK1, we examined T410 phosphorylation on Akt2R-PKMζ following insulin treatment. The data in Figure 8(D) show no change in p410 levels of transfected YFP-Akt2R-PKMζ in response to insulin (within a detection limit of ± 20% S.E.M. for immunoblotting quantified after four independent experiments) yet dramatic increases in p308 levels of transfected YFP-Akt2. These results reveal that the catalytic domain of PKCζ does not exhibit agonist-induced activity nor agonist-induced phosphorylation at the activation loop even if dragged to a location that causes Akt to be activated and phosphorylated at its activation loop.

DISCUSSION

On the kinome tree, atypical PKCs occupy a position on the AGC branch that lies between Akt and conventional PKCs [25]. Here we show that the atypical PKCζ maintains some properties unique to Akt and other properties unique to conventional PKCs, placing aPKCs at the crossroads of regulatory mechanisms for these two different families of lipid second messenger-regulated kinases. Notably, regulation of the turn motif follows the same mechanism as that for Akt: co-translational phosphorylation by ribosome-associated mTORC2. In contrast, activation loop phosphorylation at T410 follows the same mechanism as that for conventional PKCs: post-translational, constitutive phosphorylation by PDK1, concurring with previous studies that have shown constitutive phosphorylation at T410 for the short transcript PKMζ [74], and no change in p410 on purified PKCζ when treated *in vitro* with recombinant PDK1 [75]. Thus, unlike Akt but like conventional PKC, aPKCs are constitutively phosphorylated, but differ in that the first phosphorylation occurs co-translationally at the ribosome rather than post-translationally on a membrane compartment. Coupled with their lack of regulation by diacylglycerol, these results suggest that aPKCs should be considered as a separate family of kinases from the cPKCs and nPKCs.

Previous reports have suggested that aPKC autophosphorylates at the turn motif [35,76]. More recently, this site has been shown to be phosphorylated by mTORC2 *in vitro* and that phosphorylation of this site in cells depends on the integrity of mTORC2 with dephosphorylation occurring within 24 h of mTOR inhibition via Torin 1 treatment [39]. Here we show that a construct of aPKC (V266F) that maintains a native kinase domain fold but is incapable of binding ATP [58] is phosphorylated to the same level as the WT protein. These data reveal that the turn motif is not regulated by autophosphorylation on aPKCs; rather, the site is modified as newly-synthesized polypeptide emerges from the ribosome by ribosome-associated mTORC2. This co-translational phosphorylation by mTORC2 probably accounts for why acute treatment with Torin 1 does not affect the steady-state phosphorylation at the turn motif (because the bulk PKC was previously co-translationally processed by phosphorylation) and why prolonged treatment does (because loss of p560 immunoreactivity reflects turn-over of the protein). Our data also reveal that phosphorylation of the turn motif precedes that of the activation loop, similar to the order for Akt and contrasting with the order for conventional PKCs. Also contrasting with conventional PKCs, phosphorylation of the turn motif is not required for subsequent phosphorylation of the activation loop as the T560A mutant is fully phosphorylated at the activation loop. Conversely, phosphorylation of the activation loop is not required for phosphorylation of the turn motif.

Several previous studies reveal that aPKCs are regulated by autoinhibition through their pseudosubstrate segment [23,77] as are cPKCs and nPKCs. For conventional and novel PKCs, binding of diacylglycerol and its analogues to their C1 domains releases the pseudosubstrate from the substrate-binding cavity. Although aPKCs have diacylglycerol-insensitive C1 domains, previous evidence suggests that their C1 domains contribute to autoinhibition [23,77]. In support of this, our data show that PS and PA, lipids that bind the C1 domain [59], increase the catalytic activity of PKCζ, consistent with previous studies showing activation of PKCζ by these anionic membrane lipids [78,79]. Supporting conformational changes upon anionic lipid binding, *in vitro* assays reveal that the rate of dephosphorylation of PKCζ by PP1 is increased in the presence of PS, a result observed for conventional PKCs [33]. Thus, the enhanced activity and phosphatase sensitivity of aPKC by anionic lipids probably reflects engagement of the C1 domain on membranes promoting the open conformation of aPKCs, as it does for other PKCs. Because there is no high affinity ligand of the aPKC C1 domain, this interaction with anionic lipids is unlikely to provide any regulation beyond possibly stabilizing the open conformation of any aPKC scaffolded near membranes.

Akt and aPKC both exhibit overlapping functions in insulin signalling, most prominently being their requirement for insulin-stimulated glucose transport as shown through knockout models [10,80]. As for Akt, the catalytic activity of aPKC is required for its effect on insulin-regulated biological functions as determined using either kinase-dead aPKC acting as a dominant negative [4,5,7–9,81–83] or aPKC inhibitors [4,5,7,83,84], both of which impair insulin-stimulated glucose transport. However, the pathophysiological modulation of Akt vs aPKC displays tissue-dependent differences, suggesting that the regulation of these enzymes is divergent even if they exhibit similar functions. Akt is defective in the livers of diabetic mice and humans yet aPKC is hyperactive in these hepatic tissues [15,16] while

remaining dysfunctional in diabetic skeletal muscle [12,13]. Our data show that the canonical mechanism of activation for Akt involving agonist-evoked phosphorylation facilitated by PIP_3 production by PI3-K in response to growth factors is not the mechanism of activation for aPKC. In all of the cell types studied, no significant increase in activation loop phosphorylation at T410 on PKCζ was ever observed following insulin treatment as assessed using a phospho-specific antibody that does not detect a T410A mutant. Yet under the same conditions and in the same cells, dramatic increases in activation loop phosphorylation at T308 on Akt were observed. Most strikingly, forced insulin-dependent recruitment of PKCζ by replacement of its regulatory moiety with the PH domain of Akt did not cause any change in the T410 phosphorylation or catalytic activity. Concurrently, addition of the phosphatase inhibitor calyculin did not result in increased phosphorylation at either of the two priming sites, but did cause an increase in the activation loop phosphorylation of S6K. Although it is possible the T410 site is dephosphorylated by calyculin-insensitive phosphatases, 2D gel analysis reveals that a substantial amount of PKCζ is modified by phosphorylation at two sites. Additionally, treatment of cells with the PI3-K inhibitor LY294002 (LY) had no effect on the phosphorylation of T410 when treated within a time frame (20 min) that effectively blocked the insulin-induced phosphorylation of Akt at T308. A recent study reported a moderate reduction in basal phosphorylation of T410 with no change in phosphorylation of T560 following 60 min treatment with an increased dosage of LY (30 μM, [39]). This could reflect off-target effects of more prolonged LY treatment that are potentially affecting T410 phosphorylation through an indirect route not involving the canonical PI3-K/Akt pathway. Thus, insulin acutely regulates the location, phosphorylation, and global activity of Akt but has no detectable effect on any of these parameters for aPKC.

Live cell imaging studies also revealed no insulin-stimulated activity of aPKC. In contrast, insulin stimulated robust activation of Akt as assessed using the Akt activity reporter, BKAR. Correspondingly, we did not observe insulin-dependent translocation of PKCζ to the PM under conditions that caused readily detectable PM translocation of Akt and the chimaeric kinase Akt2R-PKMζ that contains the PIP_3-binding PH domain. These data indicate that the production of PIP_3 by agonist-evoked PI3-K activity does not affect PKCζ to change its proximity relative to membrane-bound PIP_3. By not reaching PIP_3 or the PM where other growth factor-stimulated lipids may be present, PKCζ cannot undergo the conformational change to relieve autoinhibition that occurs for Akt to yield activity as suggested recently [76]. We also show that no increase in the specific activity measured *in vitro* occurs for PKCζ immunoprecipitated from cells treated with insulin compared with no insulin. This observation contrasts with early studies reporting insulin-dependent increases in PKCζ activity [6,35] and supports other studies showing no increases in activity of PKCζ immunoprecipitated from insulin-treated cells [39,85] along with no increases in the phosphorylation of T410 for either tagged or endogenous PKCζ [39–41].

The lack of insulin-induced changes in aPKC location, phosphorylation or activity begs the question of how aPKCs transduce the insulin signal. We have recently shown that an acidic surface on the PB1 domain of the scaffold p62 tethers the basic pseudosubstrate of bound aPKCs to maintain the enzyme in an open and active conformation [24]. Similarly, another scaffold, PAR6 has been shown to lock aPKC in an open and active conformation [23] and

to facilitate its phosphorylation of localized substrates such as PAR3 and Lgl1 [86–90]. Given the exceptionally low catalytic rate of PKCζ (5 mol phosphate/min per mol PKC) in our study and 42 mol phosphate per min per mol PKC with MBP substrate reported previously [78], compared with cPKCs (200 mol phosphate per min per mol PKC) [57], it is likely that coordination of the enzyme next to substrates on protein scaffolds drives its signalling. By this mechanism, the constitutive presence of aPKC on scaffolds allows it to phosphorylate substrates that may be recruited to these scaffolds in an insulin-dependent manner, thus mediating the biological functions of insulin signalling such as induced glucose transport. Thus, the aPKC-regulating mechanism may derive from the insulin dependence of substrate recruitment or substrate conformation. This model is analogous to the regulation of PDK1 signalling: the enzyme is constitutively active but substrate phosphorylation is dictated by substrate conformation or accessibility [91].

The foregoing data reveal that PKCζ is primed by phosphorylation to yield a constitutively-phosphorylated, catalytically-active enzyme. First, the enzyme is co-translationally phosphorylated at the ribosome by mTORC2, followed by phosphorylation at the activation loop by PDK1. Phosphorylation at both sites is required for catalytic activity. Phosphorylations are relatively stable and insensitive to agonists such as insulin or levels of PIP_3. Although the activity of kinase moiety PKMζ is readily detectable using the genetically-encoded activity reporter CKAR, insulin-stimulated global PKCζ activity on this cytosolic substrate reporter cannot be detected. Our data support a model in which the coordination of aPKCs next to substrates on protein scaffolds drives the biological function for this class of PKC enzymes.

Acknowledgments

We thank Emily Kang for technical assistance with protein purification.

FUNDING

This work was supported by the National Institute of Health [grant numbers P01DK054441 (to A.C.N.), 1R21CA169849 (to S.F.D.) and CA154674 (to E.J.)]; and I.S.T. was supported in part by the UCSD Graduate Training Program in Cellular and Molecular Pharmacology through Institutional Training Grant T32 GM007752 from the NIGMS, National Institutes of Health.

Abbreviations

Akt	protein kinase B
aPKC	atypical protein kinase C
BKAR	B-kinase activity reporter
CHO-IR	Chinese hamster ovary cell overexpressing insulin receptor
CKAR	C-kinase activity reporter
cPKC	conventional protein kinase C
HA	haemagglutinin
IEF	isoelectric focusing

IP	immunoprecipitation
MBP	myelin basic protein
MEF	murine embryonic fibroblast
mTORC2	mammalian target of rapamycin complex 2
nPKC	novel protein kinase C
NT	no treatment
PA	phosphatidic acid
PDB	Protein Data Bank
PDK1	phosphoinositide-dependent kinase-1
PH domain	pleckstrin homology domain
PI3-K	phosphoinositide 3-kinase
PIP_2	phosphatidylinositol-4,5-biphosphate
PIP_3	phosphatidylinositol-3,4,5-triphosphate
PM	plasma membrane
PP1	protein phosphatase 1
PS	phosphatidylserine
S6K	ribosomal protein S6 kinase
Sin1	stress-activated map kinase-interacting protein 1
WT	wild-type
YFP	yellow fluorescent protein.

References

1. Farese RV, Sajan MP, Standaert ML. Insulin-sensitive protein kinases (atypical protein kinase C and protein kinase B/Akt): actions and defects in obesity and type II diabetes. Exp Biol Med. 2005; 230:593–605.
2. Farese RV, Sajan MP. Atypical protein kinase C in cardiometabolic abnormalities. Curr Opin Lipidol. 2012; 23:175–181. [PubMed: 22449812]
3. Farese RV. Function and dysfunction of aPKC isoforms for glucose transport in insulin-sensitive and insulin-resistant states. Am J Physiol Endocrinol Metabol. 2002; 283:E1–E11.
4. Bandyopadhyay G, Standaert ML, Zhao L, Yu B, Avignon A, Galloway L, Karnam P, Moscat J, Farese RV. Activation of protein kinase C (alpha, beta, and zeta) by insulin in 3T3/L1 cells. Transfection studies suggest a role for PKC-zeta in glucose transport. J Biol Chem. 1997; 272:2551–2558. [PubMed: 8999972]
5. Bandyopadhyay G, Standaert ML, Galloway L, Moscat J, Farese RV. Evidence for involvement of protein kinase C (PKC)-zeta and noninvolvement of diacylglycerol-sensitive PKCs in insulin-stimulated glucose transport in L6 myotubes. Endocrinology. 1997; 138:4721–4731. [PubMed: 9348199]
6. Standaert ML, Bandyopadhyay G, Perez L, Price D, Galloway L, Poklepovic A, Sajan MP, Cenni V, Sirri A, Moscat J, et al. Insulin activates protein kinases C-zeta and C-lambda by an

autophosphorylation-dependent mechanism and stimulates their translocation to GLUT4 vesicles and other membrane fractions in rat adipocytes. J Biol Chem. 1999; 274:25308–25316. [PubMed: 10464256]

7. Bandyopadhyay G, Sajan MP, Kanoh Y, Standaert ML, Quon MJ, Lea-Currie R, Sen A, Farese RV. PKC-zeta mediates insulin effects on glucose transport in cultured preadipocyte-derived human adipocytes. J Clin Endocrinol Metab. 2002; 87:716–723. [PubMed: 11836310]
8. Bandyopadhyay G, Standaert ML, Kikkawa U, Ono Y, Moscat J, Farese RV. Effects of transiently expressed atypical (zeta, lambda), conventional (alpha, beta) and novel (delta, epsilon) protein kinase C isoforms on insulin-stimulated translocation of epitope-tagged GLUT4 glucose transporters in rat adipocytes: specific interchangeable effects of protein kinases C-zeta and C-lambda. Biochem J. 1999; 337(Pt 3):461–470. [PubMed: 9895289]
9. Bandyopadhyay G, Kanoh Y, Sajan MP, Standaert ML, Farese RV. Effects of adenoviral gene transfer of wild-type, constitutively active, and kinase-defective protein kinase C-lambda on insulin-stimulated glucose transport in L6 myotubes. Endocrinology. 2000; 141:4120–4127. [PubMed: 11089544]
10. Bandyopadhyay G, Standaert ML, Sajan MP, Kanoh Y, Miura A, Braun U, Kruse F, Leitges M, Farese RV. Protein kinase C-lambda knockout in embryonic stem cells and adipocytes impairs insulin-stimulated glucose transport. Mol Endocrinol. 2004; 18:373–383. [PubMed: 14615604]
11. Farese RV, Sajan MP, Yang H, Li P, Mastorides S, Gower WR Jr, Nimal S, Choi CS, Kim S, Shulman GI, et al. Muscle-specific knockout of PKC-lambda impairs glucose transport and induces metabolic and diabetic syndromes. J Clin Invest. 2007; 117:2289–2301. [PubMed: 17641777]
12. Beeson M, Sajan MP, Dizon M, Grebenev D, Gomez-Daspet J, Miura A, Kanoh Y, Powe J, Bandyopadhyay G, Standaert ML, Farese RV. Activation of protein kinase C-zeta by insulin and phosphatidylinositol-3,4,5-(PO4)3 is defective in muscle in type 2 diabetes and impaired glucose tolerance: amelioration by rosiglitazone and exercise. Diabetes. 2003; 52:1926–1934. [PubMed: 12882907]
13. Kim YB, Kotani K, Ciaraldi TP, Henry RR, Kahn BB. Insulin-stimulated protein kinase C lambda/zeta activity is reduced in skeletal muscle of humans with obesity and type 2 diabetes: reversal with weight reduction. Diabetes. 2003; 52:1935–1942. [PubMed: 12882908]
14. Sajan MP, Standaert ML, Miura A, Bandyopadhyay G, Vollenweider P, Franklin DM, Lea-Currie R, Farese RV. Impaired activation of protein kinase C-zeta by insulin and phosphatidylinositol-3,4,5-(PO4)3 in cultured preadipocyte-derived adipocytes and myotubes of obese subjects. J Clin Endocrinol Metab. 2004; 89:3994–3998. [PubMed: 15292339]
15. Standaert ML, Sajan MP, Miura A, Kanoh Y, Chen HC, Farese RV Jr, Farese RV. Insulin-induced activation of atypical protein kinase C, but not protein kinase B, is maintained in diabetic (ob/ob and Goto-Kakazaki) liver. Contrasting insulin signaling patterns in liver versus muscle define phenotypes of type 2 diabetic and high fat-induced insulin-resistant states. J Biol Chem. 2004; 279:24929–24934. [PubMed: 15069067]
16. Sajan MP, Farese RV. Insulin signalling in hepatocytes of humans with type 2 diabetes: excessive production and activity of protein kinase C-iota (PKC-iota) and dependent processes and reversal by PKC-iota inhibitors. Diabetologia. 2012; 55:1446–1457. [PubMed: 22349071]
17. Sajan MP, Standaert ML, Rivas J, Miura A, Kanoh Y, Soto J, Taniguchi CM, Kahn CR, Farese RV. Role of atypical protein kinase C in activation of sterol regulatory element binding protein-1c and nuclear factor kappa B (NFkappaB) in liver of rodents used as a model of diabetes, and relationships to hyperlipidaemia and insulin resistance. Diabetologia. 2009; 52:1197–1207. [PubMed: 19357831]
18. Matsumoto M, Ogawa W, Akimoto K, Inoue H, Miyake K, Furukawa K, Hayashi Y, Iguchi H, Matsuki Y, Hiramatsu R, et al. PKClambda in liver mediates insulin-induced SREBP-1c expression and determines both hepatic lipid content and overall insulin sensitivity. J Clin Invest. 2003; 112:935–944. [PubMed: 12975478]
19. Pu Y, Peach ML, Garfield SH, Wincovitch S, Marquez VE, Blumberg PM. Effects on ligand interaction and membrane translocation of the positively charged arginine residues situated along the C1 domain binding cleft in the atypical protein kinase C isoforms. J Biol Chem. 2006; 281:33773–33788. [PubMed: 16950780]

20. Kazanietz MG, Bustelo XR, Barbacid M, Kolch W, Mischak H, Wong G, Pettit GR, Bruns JD, Blumberg PM. Zinc finger domains and phorbol ester pharmacophore. Analysis of binding to mutated form of protein kinase C zeta and the vav and c-raf proto-oncogene products. J Biol Chem. 1994; 269:11590–11594. [PubMed: 8157692]
21. Newton AC. Protein kinase C: structural and spatial regulation by phosphorylation, cofactors, and macromolecular interactions. Chem Rev. 2001; 101:2353–2364. [PubMed: 11749377]
22. Newton AC. Protein kinase C: poised to signal. Am J Physiol Endocrinol Metab. 2010; 298:E395–E402. [PubMed: 19934406]
23. Graybill C, Wee B, Atwood SX, Prehoda KE. Partitioning-defective protein 6 (Par-6) activates atypical protein kinase C (aPKC) by pseudosubstrate displacement. J Biol Chem. 2012; 287:21003–21011. [PubMed: 22544755]
24. Tsai LC, Xie L, Dore K, Xie L, Del Rio JC, King CC, Martinez-Ariza G, Hulme C, Malinow R, Bourne PE, et al. Zeta inhibitory peptide disrupts electrostatic interactions that maintain atypical protein kinase C in its active conformation on the scaffold p62. J Biol Chem. 2015; 290:21845–21856. [PubMed: 26187466]
25. Manning G, Whyte DB, Martinez R, Hunter T, Sudarsanam S. The protein kinase complement of the human genome. Science. 2002; 298:1912–1934. [PubMed: 12471243]
26. Gao T, Furnari F, Newton AC. PHLPP: a phosphatase that directly dephosphorylates Akt, promotes apoptosis, and suppresses tumor growth. Mol Cell. 2005; 18:13–24. [PubMed: 15808505]
27. Gao T, Brognard J, Newton AC. The phosphatase PHLPP controls the cellular levels of protein kinase C. J Biol Chem. 2008; 283:6300–6311. [PubMed: 18162466]
28. Edwards AS, Newton AC. Phosphorylation at conserved carboxyl-terminal hydrophobic motif regulates the catalytic and regulatory domains of protein kinase C. J Biol Chem. 1997; 272:18382–18390. [PubMed: 9218480]
29. Bornancin F, Parker PJ. Phosphorylation of protein kinase C-alpha on serine 657 controls the accumulation of active enzyme and contributes to its phosphatase-resistant state. J Biol Chem. 1997; 272:3544–3549. [PubMed: 9013603]
30. Dutil EM, Toker A, Newton AC. Regulation of conventional protein kinase C isozymes by phosphoinositide-dependent kinase 1 (PDK-1). Curr Biol. 1998; 8:1366–1375. [PubMed: 9889098]
31. Le Good JA, Ziegler WH, Parekh DB, Alessi DR, Cohen P, Parker PJ. Protein kinase C isotypes controlled by phosphoinositide 3-kinase through the protein kinase PDK1. Science. 1998; 281:2042–2045. [PubMed: 9748166]
32. Chou MM, Hou W, Johnson J, Graham LK, Lee MH, Chen CS, Newton AC, Schaffhausen BS, Toker A. Regulation of protein kinase C zeta by PI 3-kinase and PDK-1. Curr Biol. 1998; 8:1069–1077. [PubMed: 9768361]
33. Dutil EM, Keranen LM, DePaoli-Roach AA, Newton AC. *In vivo* regulation of protein kinase C by trans-phosphorylation followed by autophosphorylation. J Biol Chem. 1994; 269:29359–29362. [PubMed: 7961910]
34. Bandyopadhyay G, Standaert ML, Sajan MP, Karnitz LM, Cong L, Quon MJ, Farese RV. Dependence of insulin-stimulated glucose transporter 4 translocation on 3-phosphoinositide-dependent protein kinase-1 and its target threonine-410 in the activation loop of protein kinase C-zeta. Mol Endocrinol. 1999; 13:1766–1772. [PubMed: 10517677]
35. Standaert ML, Bandyopadhyay G, Kanoh Y, Sajan MP, Farese RV. Insulin and PIP3 activate PKC-zeta by mechanisms that are both dependent and independent of phosphorylation of activation loop (T410) and autophosphorylation (T560) sites. Biochemistry. 2001; 40:249–255. [PubMed: 11141077]
36. Hirai T, Chida K. Protein kinase Czeta (PKCzeta): activation mechanisms and cellular functions. J Biochem. 2003; 133:1–7. [PubMed: 12761192]
37. Alessi DR, Andjelkovic M, Caudwell B, Cron P, Morrice N, Cohen P, Hemmings BA. Mechanism of activation of protein kinase B by insulin and IGF-1. EMBO J. 1996; 15:6541–6551. [PubMed: 8978681]

38. Alessi DR, James SR, Downes CP, Holmes AB, Gaffney PR, Reese CB, Cohen P. Characterization of a 3-phosphoinositide-dependent protein kinase which phosphorylates and activates protein kinase Balpha. Curr Biol. 1997; 7:261–269. [PubMed: 9094314]
39. Li X, Gao T. mTORC2 phosphorylates protein kinase Czeta to regulate its stability and activity. EMBO Rep. 2014; 15:191–198. [PubMed: 24375676]
40. Chen W, Goff MR, Kuang H, Chen G. Higher protein kinase C zeta in fatty rat liver and its effect on insulin actions in primary hepatocytes. PloS One. 2015; 10:e0121890. [PubMed: 25822413]
41. Frosig C, Sajan MP, Maarbjerg SJ, Brandt N, Roepstorff C, Wojtaszewski JF, Kiens B, Farese RV, Richter EA. Exercise improves phosphatidylinositol-3,4,5-trisphosphate responsiveness of atypical protein kinase C and interacts with insulin signalling to peptide elongation in human skeletal muscle. J Physiol. 2007; 582(Pt 3):1289–1301. [PubMed: 17540697]
42. Hauge C, Antal TL, Hirschberg D, Doehn U, Thorup K, Idrissova L, Hansen K, Jensen ON, Jørgensen TJ, Biondi RM, Frödin M. Mechanism for activation of the growth factor-activated AGC kinases by turn motif phosphorylation. EMBO J. 2007; 26:2251–2261. [PubMed: 17446865]
43. Bornancin F, Parker PJ. Phosphorylation of threonine 638 critically controls the dephosphorylation and inactivation of protein kinase Calpha. Curr Biol. 1996; 6:1114–1123. [PubMed: 8805373]
44. Edwards AS, Faux MC, Scott JD, Newton AC. Carboxyl-terminal phosphorylation regulates the function and subcellular localization of protein kinase C betaII. J Biol Chem. 1999; 274:6461–6468. [PubMed: 10037738]
45. Facchinetti V, Ouyang W, Wei H, Soto N, Lazorchak A, Gould C, Lowry C, Newton AC, Mao Y, Miao RQ, et al. The mammalian target of rapamycin complex 2 controls folding and stability of Akt and protein kinase C. EMBO J. 2008; 27:1932–1943. [PubMed: 18566586]
46. Ikenoue T, Inoki K, Yang Q, Zhou X, Guan KL. Essential function of TORC2 in PKC and Akt turn motif phosphorylation, maturation and signalling. EMBO J. 2008; 27:1919–1931. [PubMed: 18566587]
47. Oh WJ, Wu CC, Kim SJ, Facchinetti V, Julien LA, Finlan M, Roux PP, Su B, Jacinto E. mTORC2 can associate with ribosomes to promote cotranslational phosphorylation and stability of nascent Akt polypeptide. EMBO J. 2010; 29:3939–3951. [PubMed: 21045808]
48. Zinzalla V, Stracka D, Oppliger W, Hall MN. Activation of mTORC2 by association with the ribosome. Cell. 2011; 144:757–768. [PubMed: 21376236]
49. Borner C, Filipuzzi I, Wartmann M, Eppenberger U, Fabbro D. Biosynthesis and posttranslational modifications of protein kinase C in human breast cancer cells. J Biol Chem. 1989; 264:13902–13909. [PubMed: 2474538]
50. Dutil EM, Newton AC. Dual role of pseudosubstrate in the coordinated regulation of protein kinase C by phosphorylation and diacylglycerol. J Biol Chem. 2000; 275:10697–10701. [PubMed: 10744767]
51. Guertin DA, Stevens DM, Thoreen CC, Burds AA, Kalaany NY, Moffat J, Brown M, Fitzgerald KJ, Sabatini DM. Ablation in mice of the mTORC components raptor, rictor, or mLST8 reveals that mTORC2 is required for signaling to Akt-FOXO and PKCalpha, but not S6K1. Dev Cell. 2006; 11:859–871. [PubMed: 17141160]
52. Behn-Krappa A, Newton AC. The hydrophobic phosphorylation motif of conventional protein kinase C is regulated by autophosphorylation. Curr Biol. 1999; 9:728–737. [PubMed: 10421574]
53. Violin JD, Zhang J, Tsien RY, Newton AC. A genetically encoded fluorescent reporter reveals oscillatory phosphorylation by protein kinase C. J Cell Biol. 2003; 161:899–909. [PubMed: 12782683]
54. Kunkel MT, Ni Q, Tsien RY, Zhang J, Newton AC. Spatio-temporal dynamics of protein kinase B/Akt signaling revealed by a genetically encoded fluorescent reporter. J Biol Chem. 2005; 280:5581–5587. [PubMed: 15583002]
55. Ezhevsky SA, Ho A, Becker-Hapak M, Davis PK, Dowdy SF. Differential regulation of retinoblastoma tumor suppressor protein by G(1) cyclin-dependent kinase complexes *in vivo*. Mol Cell Biol. 2001; 21:4773–4784. [PubMed: 11416152]
56. Wu-Zhang AX, Murphy AN, Bachman M, Newton AC. Isozyme-specific interaction of protein kinase Cdelta with mitochondria dissected using live cell fluorescence imaging. J Biol Chem. 2012; 287:37891–37906. [PubMed: 22988234]

57. Johnson JE, Edwards AS, Newton AC. A putative phosphatidylserine binding motif is not involved in the lipid regulation of protein kinase C. J Biol Chem. 1997; 272:30787–30792. [PubMed: 9388219]
58. Taylor SS, Shaw A, Hu J, Meharena HS, Kornev A. Pseudokinases from a structural perspective. Biochem Soc Trans. 2013; 41:981–986. [PubMed: 23863167]
59. Johnson JE, Giorgione J, Newton AC. The C1 and C2 domains of protein kinase C are independent membrane targeting modules, with specificity for phosphatidylserine conferred by the C1 domain. Biochemistry. 2000; 39:11360–11369. [PubMed: 10985781]
60. Orr JW, Newton AC. Interaction of protein kinase C with phosphatidylserine. 2 Specificity and regulation. Biochemistry. 1992; 31:4667–4673. [PubMed: 1581317]
61. Orr JW, Newton AC. Interaction of protein kinase C with phosphatidylserine. 1 Cooperativity in lipid binding. Biochemistry. 1992; 31:4661–4667. [PubMed: 1581316]
62. Bell RM, Hannun Y, Loomis C. Mixed micelle assay of protein kinase C. Methods Enzymol. 1986; 124:353–359. [PubMed: 3520216]
63. Hannun YA, Loomis CR, Bell RM. Protein kinase C activation in mixed micelles. Mechanistic implications of phospholipid, diacylglycerol, and calcium interdependencies. J Biol Chem. 1986; 261:7184–7190. [PubMed: 3711083]
64. Newton AC, Koshland DE Jr. Phosphatidylserine affects specificity of protein kinase C substrate phosphorylation and autophosphorylation. Biochemistry. 1990; 29:6656–6661. [PubMed: 2397206]
65. Sabatini DM. mTOR and cancer: insights into a complex relationship. Nat Rev Cancer. 2006; 6:729–734. [PubMed: 16915295]
66. Pearson RB, Dennis PB, Han JW, Williamson NA, Kozma SC, Wettenhall RE, Thomas G. The principal target of rapamycin-induced p70s6k inactivation is a novel phosphorylation site within a conserved hydrophobic domain. EMBO J. 1995; 14:5279–5287. [PubMed: 7489717]
67. Wu-Zhang AX, Schramm CL, Nabavi S, Malinow R, Newton AC. Cellular pharmacology of protein kinase Mzeta (PKMzeta) contrasts with its *in vitro* profile: implications for PKMzeta as a mediator of memory. J Biol Chem. 2012; 287:12879–12885. [PubMed: 22378786]
68. Standaert ML, Galloway L, Karnam P, Bandyopadhyay G, Moscat J, Farese RV. Protein kinase C-zeta as a downstream effector of phosphatidylinositol 3-kinase during insulin stimulation in rat adipocytes., Potential role in glucose transport. J Biol Chem. 1997; 272:30075–30082. [PubMed: 9374484]
69. Akimoto K, Takahashi R, Moriya S, Nishioka N, Takayanagi J, Kimura K, Fukui Y, Osada Si, Mizuno K, Hirai Si, et al. EGF or PDGF receptors activate atypical PKClambda through phosphatidylinositol 3-kinase. EMBO J. 1996; 15:788–798. [PubMed: 8631300]
70. Antal CE, Violin JD, Kunkel MT, Skovso S, Newton AC. Intramolecular conformational changes optimize protein kinase C signaling. Chem Biol. 2014; 21:459–469. [PubMed: 24631122]
71. Andjelkovic M, Alessi DR, Meier R, Fernandez A, Lamb NJ, Frech M, Cron P, Cohen P, Lucocq JM, Hemmings BA. Role of translocation in the activation and function of protein kinase B. J Biol Chem. 1997; 272:31515–31524. [PubMed: 9395488]
72. Bellacosa A, Chan TO, Ahmed NN, Datta K, Malstrom S, Stokoe D, McCormick F, Feng J, Tsichlis P. Akt activation by growth factors is a multiple-step process: the role of the PH domain. Oncogene. 1998; 17:313–325. [PubMed: 9690513]
73. Trujillo JI, Kiefer JR, Huang W, Thorarensen A, Xing L, Caspers NL, Day JE, Mathis KJ, Kretzmer KK, Reitz BA, et al. 2-(6-Phenyl-1H-indazol-3-yl)-1H-benzo[d]imidazoles: design and synthesis of a potent and isoform selective PKC-zeta inhibitor. Bioorg Med Chem Lett. 2009; 19:908–911. [PubMed: 19097791]
74. Kelly MT, Crary JF, Sacktor TC. Regulation of protein kinase Mzeta synthesis by multiple kinases in long-term potentiation. J Neurosci. 2007; 27:3439–3444. [PubMed: 17392460]
75. Smith L, Wang Z, Smith JB. Caspase processing activates atypical protein kinase C zeta by relieving autoinhibition and destabilizes the protein. Biochem J. 2003; 375(Pt 3):663–671. [PubMed: 12887331]

76. Ivey RA, Sajan MP, Farese RV. Requirements for pseudosubstrate arginine residues during auto-inhibition and phosphatidylinositol-3,4,5-(PO4)3-dependent activation of atypical PKC. J Biol Chem. 2014; 289:25021–25030. [PubMed: 25035426]
77. Lopez-Garcia LA, Schulze JO, Frohner W, Zhang H, Suss E, Weber N, Navratil J, Amon S, Hindie V, Zeuzem S, et al. Allosteric regulation of protein kinase PKCzeta by the N-terminal C1 domain and small compounds to the PIF-pocket. Chem Biol. 2011; 18:1463–1473. [PubMed: 22118680]
78. Nakanishi H, Exton JH. Purification and characterization of the zeta isoform of protein kinase C from bovine kidney. J Biol Chem. 1992; 267:16347–16354. [PubMed: 1322899]
79. Limatola C, Schaap D, Moolenaar WH, van Blitterswijk WJ. Phosphatidic acid activation of protein kinase C-zeta overexpressed in COS cells: comparison with other protein kinase C isotypes and other acidic lipids. Biochem J. 1994; 304(Pt 3):1001–1008. [PubMed: 7818462]
80. Cho H, Mu J, Kim JK, Thorvaldsen JL, Chu Q, Crenshaw EB 3rd, Kaestner KH, Bartolomei MS, Shulman GI, Birnbaum MJ. Insulin resistance and a diabetes mellitus-like syndrome in mice lacking the protein kinase Akt2 (PKB beta). Science. 2001; 292:1728–1731. [PubMed: 11387480]
81. Braiman L, Alt A, Kuroki T, Ohba M, Bak A, Tennenbaum T, Sampson SR. Activation of protein kinase C zeta induces serine phosphorylation of VAMP2 in the GLUT4 compartment and increases glucose transport in skeletal muscle. Mol Cell Biol. 2001; 21:7852–7861. [PubMed: 11604519]
82. Kotani K, Ogawa W, Matsumoto M, Kitamura T, Sakaue H, Hino Y, Miyake K, Sano W, Akimoto K, Ohno S, Kasuga M. Requirement of atypical protein kinase clambda for insulin stimulation of glucose uptake but not for Akt activation in 3T3-L1 adipocytes. Mol Cell Biol. 1998; 18:6971–6982. [PubMed: 9819385]
83. Imamura T, Huang J, Usui I, Satoh H, Bever J, Olefsky JM. Insulin-induced GLUT4 translocation involves protein kinase C-lambda-mediated functional coupling between Rab4 and the motor protein kinesin. Mol Cell Biol. 2003; 23:4892–4900. [PubMed: 12832475]
84. Imamura T, Ishibashi K, Dalle S, Ugi S, Olefsky JM. Endothelin-1-induced GLUT4 translocation is mediated via Galpha(q/11) protein and phosphatidylinositol 3-kinase in 3T3-L1 adipocytes. J Biol Chem. 1999; 274:33691–33695. [PubMed: 10559259]
85. Tsuru M, Katagiri H, Asano T, Yamada T, Ohno S, Ogihara T, Oka Y. Role of PKC isoforms in glucose transport in 3T3-L1 adipocytes: insignificance of atypical PKC. Am J Physiol Endocrinol Metab. 2002; 283:E338–E345. [PubMed: 12110540]
86. Hung TJ, Kemphues KJ. PAR-6 is a conserved PDZ domain-containing protein that colocalizes with PAR-3 in Caenorhabditis elegans embryos. Development. 1999; 126:127–135. [PubMed: 9834192]
87. Izumi Y, Hirose T, Tamai Y, Hirai S, Nagashima Y, Fujimoto T, Tabuse Y, Kemphues KJ, Ohno S. An atypical PKC directly associates and colocalizes at the epithelial tight junction with ASIP, a mammalian homologue of Caenorhabditis elegans polarity protein PAR-3. J Cell Biol. 1998; 143:95–106. [PubMed: 9763423]
88. Joberty G, Petersen C, Gao L, Macara IG. The cell-polarity protein Par6 links Par3 and atypical protein kinase C to Cdc42. Nat Cell Biol. 2000; 2:531–539. [PubMed: 10934474]
89. Plant PJ, Fawcett JP, Lin DC, Holdorf AD, Binns K, Kulkarni S, Pawson T. A polarity complex of mPar-6 and atypical PKC binds, phosphorylates and regulates mammalian Lgl. Nat Cell Biol. 2003; 5:301–308. [PubMed: 12629547]
90. Yamanaka T, Horikoshi Y, Sugiyama Y, Ishiyama C, Suzuki A, Hirose T, Iwamatsu A, Shinohara A, Ohno S. Mammalian Lgl forms a protein complex with PAR-6 and aPKC independently of PAR-3 to regulate epithelial cell polarity. Curr Biol. 2003; 13:734–743. [PubMed: 12725730]
91. Toker A, Newton AC. Cellular signaling: pivoting around PDK-1. Cell. 2000; 103:185–188. [PubMed: 11057891]

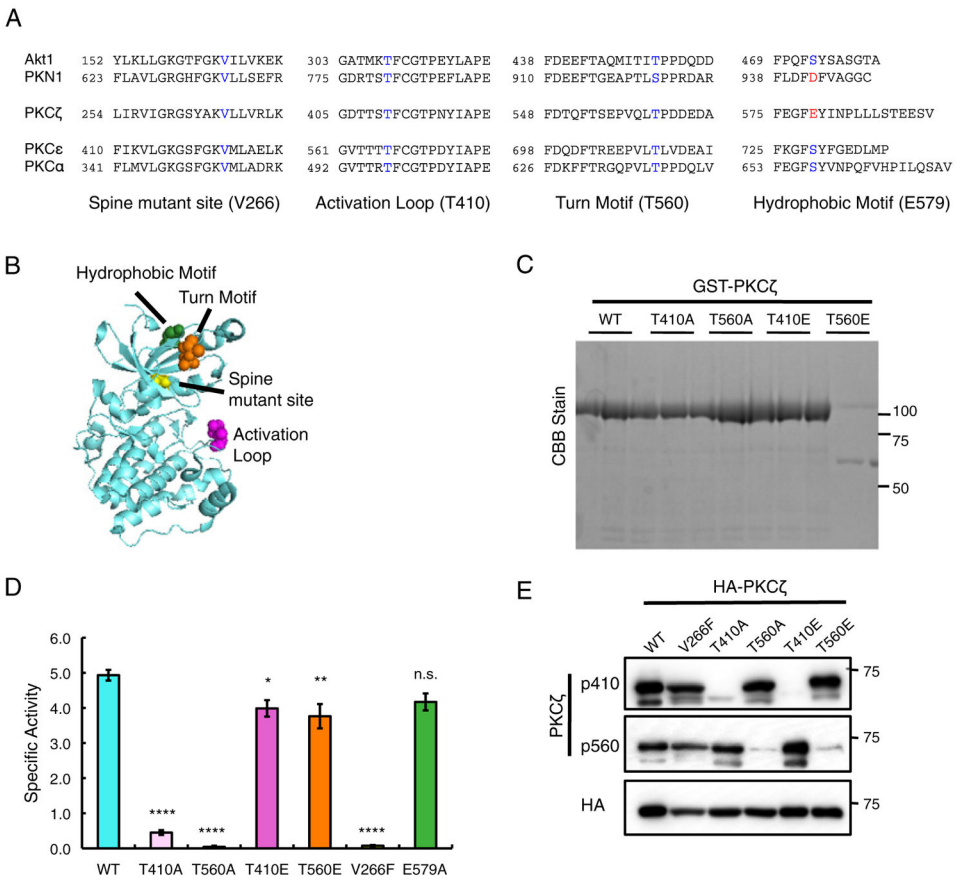

Figure 1. Phosphorylation at the activation loop and turn motif of PKCζ is each independently required but not sufficient for activity

(**A**) Alignment of amino acid residues at the spine mutant, activation loop, turn motif and hydrophobic motif sites shown in blue text for human PKC (conventional PKC*α*, novel PKC*ε* and atypical PKC*ζ*) and the other related AGC kinases Akt1 and PKN1. The hydrophobic motif Glu and Asp residues of PKC*ζ* and PKN1 are notated in red. Sequences for these kinases are listed in the order they appear on their branch of the kinome [25]. Specific residue numbers for human PKC*ζ* are indicated. (**B**) Structure of an aPKC kinase domain (human PKC*ι*, PDB: 3A8W) showing locations of analogous sites for PKC*ζ*. (**C**) Coomassie brilliant blue (CBB) stain of GST-PKC*ζ* expressed and harvested from baculoviral-infected Sf-9 cells, isolated to >90% purity. (**D**) Specific activity, measured in mol of phosphate (P) · min^{-1} · mol $PKC\zeta^{-1}$, of WT and various mutants of purified GST-PKC*ζ* incubated *in vitro* with MBP as substrate. Error bars represent ± S.E.M. for $n = 3$ reaction experiments. Statistical analysis was performed using ordinary one-way ANOVA followed by Dunnett's multiple comparison test with WT as control. Significance notated as * ($P < 0.05$), ** ($P < 0.01$), **** ($P < 0.0001$), or n.s. (not significant). (**E**) Immunoblots showing activation loop and turn motif phosphorylation status of HA-PKC*ζ* and mutants expressed in mammalian CHO-IR cells.

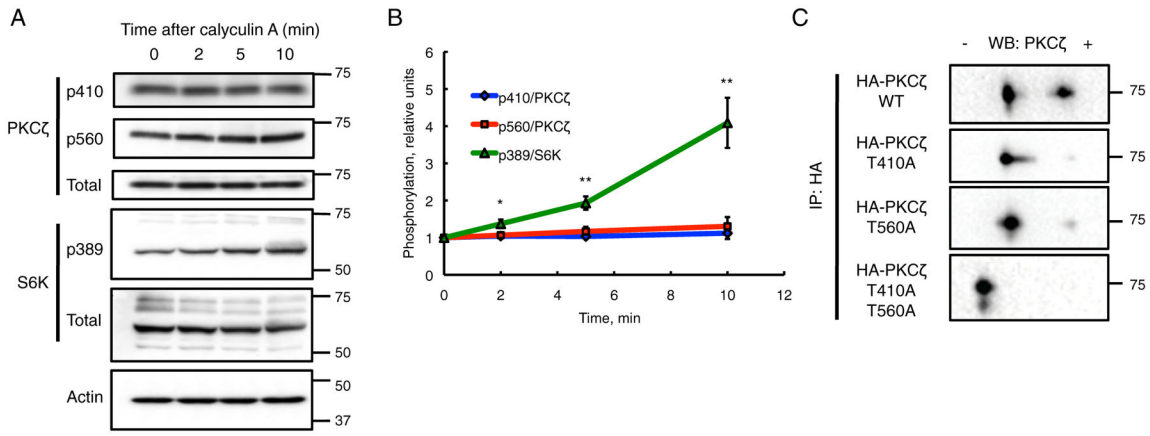

Figure 2. PKCζ is basally phosphorylated and insensitive to phosphatase inhibition

(**A**) Immunoblots of lysates from COS-7 cells treated with 50 nM calyculin A (phosphatase inhibitor) for a time course of 0–10 min showing degree of T410 and T560 phosphorylation on PKCζ over time in comparison with T389 phosphorylation on S6K. (**B**) Quantification of blots from (A) using $n = 4$ separate experiments shown as phosphorylated protein over total protein normalized to $t = 0$ min baseline, plotted as mean ± S.E.M. Statistical analysis was performed using ordinary one-way ANOVA at each time point followed by Dunnett's multiple comparison test with p389/S6K as control. Significance notated as * ($P < 0.05$) or ** ($P < 0.005$). (**C**) Immunoblots of 2D-IEF run on immunoprecipitated HA-PKCζ WT and phosphorylation site mutants.

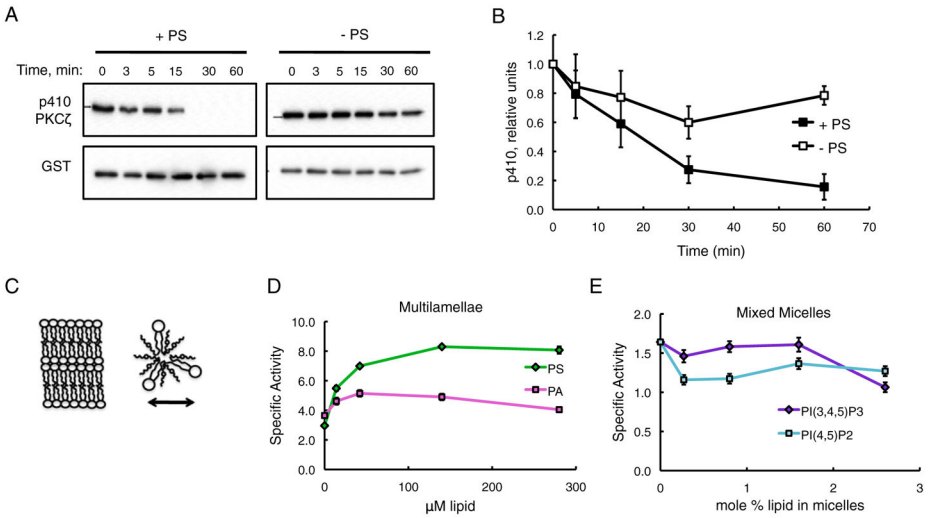

Figure 3. Phosphatidylserine promotes the open conformation of PKCζ and increases specific activity of purified PKCζ; low concentrations of phosphoinositides do not activate PKCζ

(**A**) Time course of purified GST-PKCζ and pure PP1 incubated with or without phosphatidylserine (PS) lipid. Immunoblots show degree of T410 dephosphorylation over time, with corresponding GST signal representing total GST-PKCζ present. (**B**) Quantification of blots from (A) using $n = 4$ separate experiments shown as p410 signal over GST signal normalized to $t = 0$ min baseline, plotted as mean ± S.E.M. Statistical analysis was performed using unpaired t-tests for $t = 30$ min and $t = 60$ min time points. Significance notated as ** ($P < 0.005$) or n.s. (not significant). (**C**) Diagram depicting structural presentation of lipids in multilamellar systems and Triton X-100 detergent soluble micelles. (**D**) Specific activity, measured in mol (P) · min^{-1} · mol PKCζ of purified GST-PKCζ incubated with either PS or PA multilamellar of variable lipid concentrations. (**E**) Specific activity of purified GST-PKCζ incubated with Triton X-100 mixed micelles of varying mole % lipid present for PIP_3 and PIP_2.

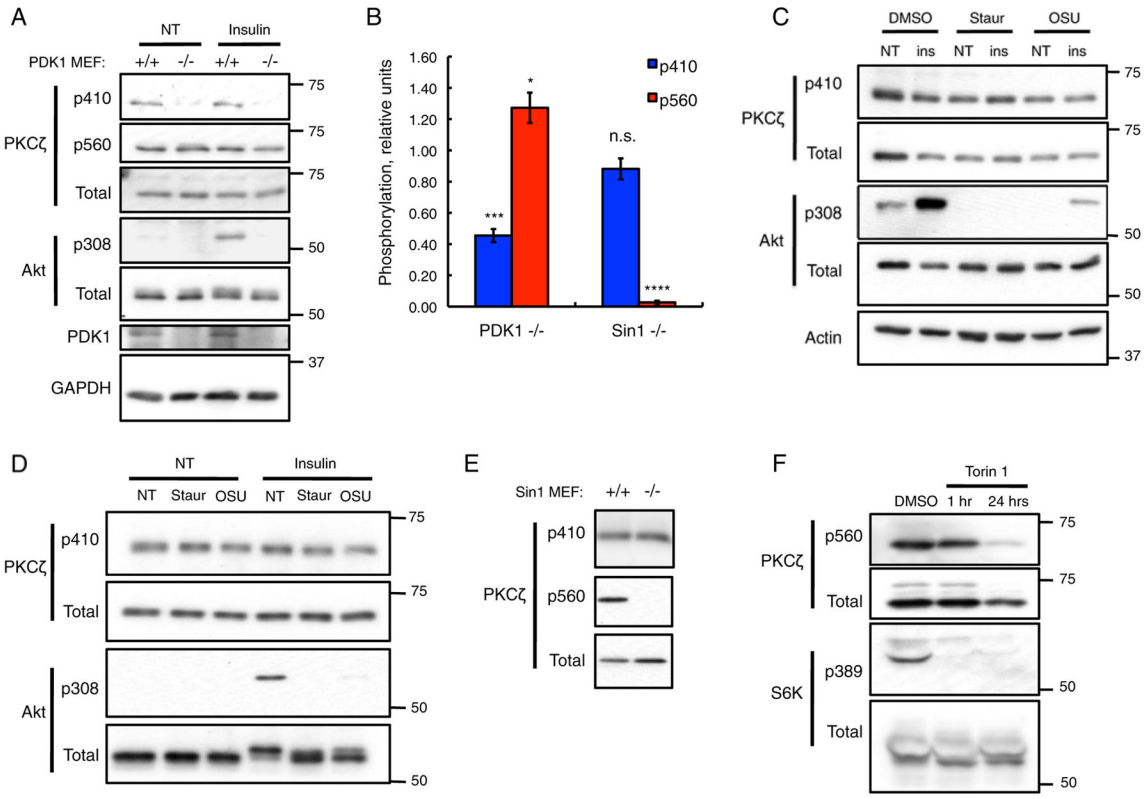

Figure 4. PDK1 and mTORC2 are required for constitutive phosphorylation of T410 and T560 sites on PKCζ, respectively

(**A**) Immunoblots of PDK1+/+ and PDK1−/− lysates comparing phosphorylation at the activation loop (p410) and turn motif (p560) sites of PKCζ along with activation loop phosphorylation of Akt (p308) with or without 100 nM insulin treatment for 10 min. (**B**) Quantification of blots from (A) and (E) using $n = 3–4$ separate experiments shown as phosphorylated protein over total protein normalized to corresponding +/+ MEFs, plotted as mean ± S.E.M. Statistical analysis was performed using ordinary one-way ANOVA followed by Dunnett's multiple comparison test with WT baseline as control. Significance notated as * ($P < 0.05$), *** ($P < 0.001$), **** ($P < 0.0001$) or n.s. (not significant). PDK1+/+ MEFs and (**C**) and CHO-IR (**D**) were serum starved overnight and treated with DMSO, 1 μM staurosporine (Staur) or 10 μM OSU03012 (OSU) for 30 min prior to treatment with or without 100 nM insulin for 10 min. Lysates were immunoblotted for activation loop phosphorylation status of PKCζ and Akt. (**E**) Immunoblots of Sin1+/+ and Sin1−/− MEFs showing phosphorylation at the activation loop and turn motif sites of PKCζ. (**F**) Immunoblots of Sin1+/+ MEFs treated with DMSO or 100 nM Torin 1 (mTOR inhibitor) for 1 h or 24 h prior to lysis showing phosphorylation of T560 on PKCζ. Phosphorylation of S6K at T389 is shown as validation of mTOR inhibition.

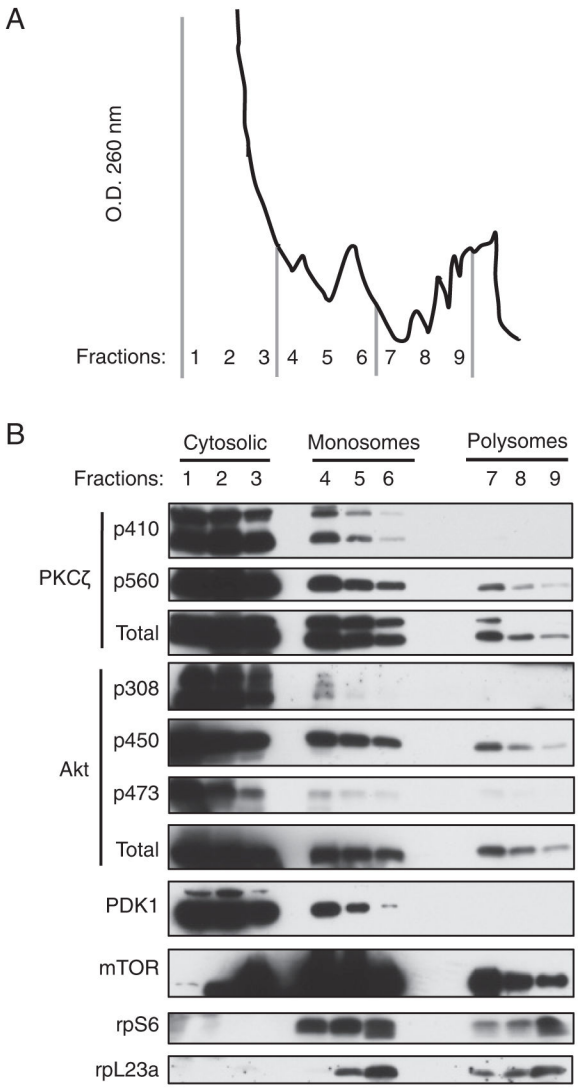

Figure 5. The turn motif site of PKCζ is phosphorylated during translation

MEFs were serum starved overnight and re-stimulated with serum for 1 h, then treated with cycloheximide for 15 min. (**A**) Absorbance (A_{260}; *y* axis) versus increasing density (x axis) of sucrose fractions from cell lysates was monitored. (**B**) Aliquots of each fraction were separated by SDS-PAGE followed by immunoblotting for analysis of protein expression and phosphorylation state of PKCζ and Akt. Ribosomal marker proteins rpS6 and rpL23a are shown for validation of fractionation process.

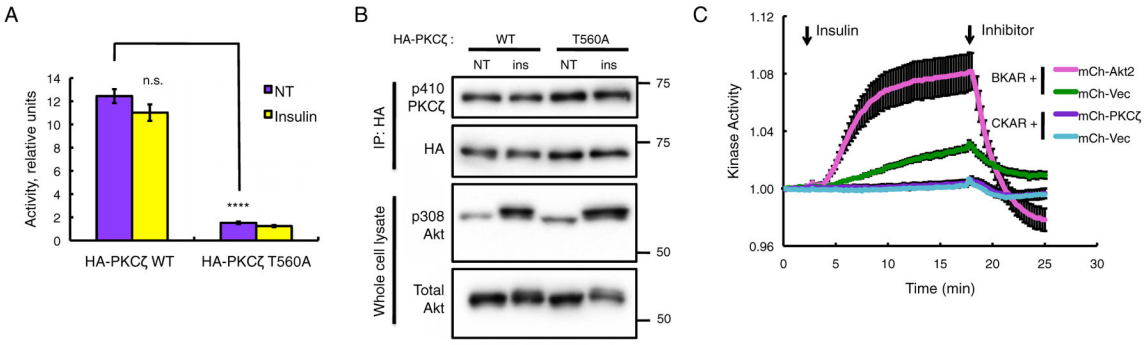

Figure 6. The catalytic activity of PKCζ does not increase due to insulin stimulation

(**A**) Activity of WT and kinase-dead (T560A) HA-PKCζ immunoprecipitated from Hep1C1C7 serum starved overnight and treated with (insulin) or without (NT, no treatment) 100 nM insulin for 10 min prior to lysis. Kinase-bound beads were incubated *in vitro* with MBP substrate and [γ-^{32}P]ATP. Activity was measured as CPM normalized by total HA signal from immunoblot and plotted as mean ± S.E.M. for $n = 3$ reaction experiments. Statistical analysis was performed using ordinary two-way ANOVA followed by Dunnett's multiple comparison test with WT NT as control. Significance notated as **** ($P < 0.0001$) or n.s. (not significant). (**B**) Immunoblots of activation loop phosphorylation for immunoprecipitated HA-PKCζ from (**A**) along with total HA signal and activation loop phosphorylation of Akt from whole cell lysate. (**C**) Global cytosolic kinase activity measured via changes in CFP over FRET ratio using Akt-specific reporter BKAR and mCherry-tagged Akt2 or vector (Vec) or PKC-specific reporter CKAR and mCherry-tagged PKCζ or vector in live COS-7 cells serum starved for 4–6 h prior to imaging and treatment with 100 nM insulin then inhibitors (20 μM GDC-0068 for BKAR assays or 1 μM staurosporine for CKAR assays). The trace for each cell imaged was normalized to its $t = 0$ min baseline value, and normalized FRET ratios were combined from three independent experiments and plotted as mean ± S.E.M.

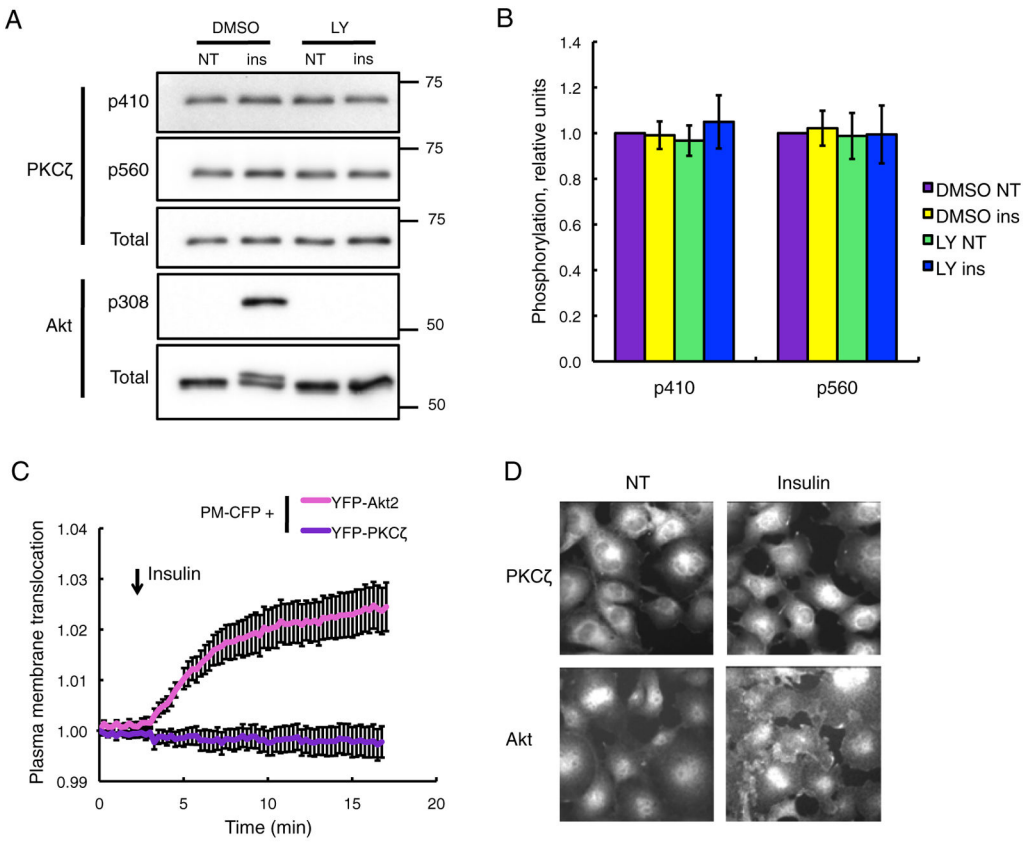

Figure 7. The phosphorylation of PKCζ is not agonist-evoked nor regulated by PI3-K through translocation to the PM in response to insulin

(**A**) Hep1C1C7 cells were serum starved for 4 h then treated with DMSO or 20 μM LY294002 (LY) for 20 min prior to treatment with or without 100 nM insulin for 10 min. Immunoblots showing phosphorylation status of PKCζ at the activation loop (p410), turn motif (p560) and Akt at the activation loop (p308). (**B**) Quantification of blots from (A) using $n = 8$ separate experiments shown as p410 or p560 over total PKCζ normalized to 'DMSO NT' control, plotted as mean ± S.E.M. (**C**) Translocation assay of YFP-tagged Akt2 or PKCζ to plasma membrane (PM-CFP) in live COS-7 cells serum starved for 4–6 h prior to imaging, measured as change in FRET over CFP ratio in response to 100 nM insulin. The trace for each cell imaged was normalized to its $t = 0$ min baseline value, and normalized FRET ratios were combined from three independent experiments and plotted as mean ± S.E.M. (**D**) Representative images of COS-7 cells treated with or without 100 nM insulin for 10 min prior to fixation and staining with antibodies for PKCζ or Akt as described in Experimental.

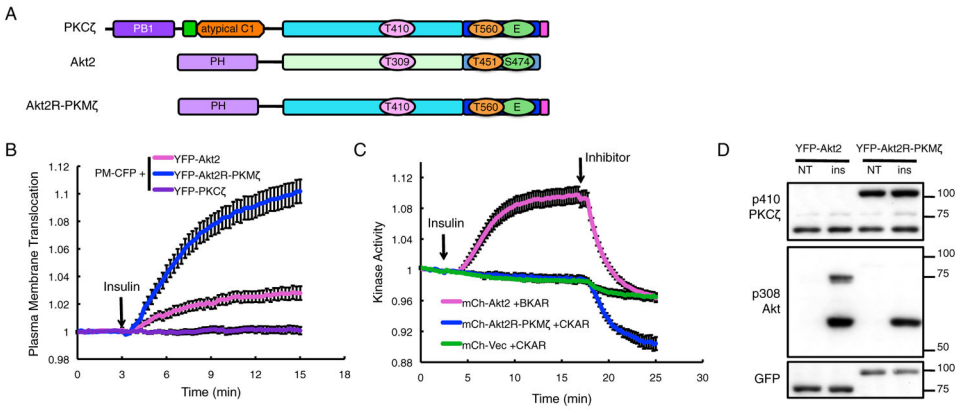

Figure 8. A fusion construct of the Akt2 PH domain with PKMζ translocates to the PM in response to insulin yet does not exhibit agonist-evoked activity or phosphorylation at the activation loop

(**A**) Schematic of the domains and phosphorylation sites present in PKCζ, Akt2 and the chimaeric kinase Akt2R-PKMζ, consisting of the PH domain of Akt2 with the catalytic moiety of PKCζ (PKMζ). (**B**) Translocation assay of YFP-tagged Akt2, Akt2R-PKMζ or PKCζ to plasma membrane (PM-CFP) in live COS-7 cells serum starved prior to imaging, measured as change in FRET over CFP ratio in response to 100 nM insulin. The trace for each cell imaged was normalized to its $t = 0$ min baseline value, and normalized FRET ratios were combined from three independent experiments and plotted as mean ± S.E.M. (**C**) Global cytosolic kinase activity measured via changes in CFP over FRET ratio using Akt-specific reporter BKAR and mCherry-tagged Akt2 or PKC-specific reporter CKAR and mCherry-tagged Akt2R-PKMζ or vector in live COS-7 cells serum starved prior to imaging and treatment with 100 nM insulin then inhibitors (20 μM GDC-0068 for BKAR assays or 5 μM PZ09 for CKAR assays). The trace for each cell imaged was normalized to its $t = 0$ min baseline value, and normalized FRET ratios were combined from three independent experiments and plotted as mean ± S.E.M. (**D**) CHO-IR cells were transfected with either YFP-Akt2 or YFP-Akt2R-PKMζ, serum starved overnight then treated with or without 100 nM insulin for 10 min. Immunoblots show phosphorylation status of Akt2R-PKMζ and Akt2 at their respective activation loops (p410 and p308). Upper bands on p410 and p308 blots indicate over-expressed YFP-tagged constructs whereas lower bands are indicative of endogenous PKCζ or Akt.